WPCA NEWS
Worldwide Pollution Control Association
www.wpca.info
A Bi-Annual News Journal Sponsored by the WPCA Winter - 2017

Executive Summary

Consequences of Selenium Behavior in Coal-Fired Boilers on FGD Wastewater Treatment

By Connie Senior and Sharon Sjostrom, ADA-ES, Inc.

Selenium is an essential micronutrient, but it can be toxic at higher doses. Selenium air emissions from coal-fired electric utility boilers in the U.S. are regulated by the Environmental Protection Agency (EPA) under the Mercury and Air Toxics Standards (MATS) rule. For a power plant, adding selenium chemistry to the mix of factors to consider further complicates operations and increases the importance of incorporating a systems perspective.

Full Story….

Wet Electrostatic Precipitator Application for Coal-fired Boiler

By Hardik Shah, Southern Environmental, Inc

Case study of the implementation of SEI's membrane wet electrostatic precipitator technology on an industrial coal fired boiler application. The membrane design addresses operational and maintenance issues common to most WESP installations.

Full Story….

Limitations in Reduced Load SCR Operation

By Joakim Reimer Thøgersen, Hans Jensen-Holm. Haldor Topsøe A/S

Increased wind-power capacity and tightened NOx regulations are an expected trend in the rest of Europe and the U.S. in the years to come. There is therefore an increased focus on operation of the SCR DeNOx units at lower loads. Haldor Topsøe's DNX® catalyst with its high porosity ensures optimal resistance against ABS condensation and combined with the Haldor Topsøe design tools, SCR DeNOx operation around the ABS dew point can be utilized to the maximum possible extent.

Full Story….

High Reactivity Hydrated Lime for Heat Rate Improvement

By Charles A. Lockert, Mississippi Lime Company

With the implementation of MATS, depressed natural gas prices and an increasing emphasis on renewables, traditional coal-fired generating assets are looking for flexible solutions to improve operating efficiency. One avenue for efficiency gains could come from a hydrated lime dry sorbent injection system -- shifting the focus of the DSI system from a regulatory need to a source of operational and overall cost benefit to the user. This paper outlines the benefits and cost implications of increasing, rather than minimizing, hydrated lime usage for overall commercial improvement.

Full Story….

Optimizing the Glenarm Station Gas Turbine OTSG Through Flow Modeling and Testing

By Kevin W. Linfield, Matthew R. Gentry, and Kanthan Rajendran, Airflow Sciences Corporation

The City of Pasadena California embarked on the $137 million "Glenarm Repowering Project" to replace the 50-year old steam generating unit with a new combined-cycle 71 MW power generating unit featuring a new gas turbine, steam turbine, once-through steam generator (OTSG). Innovative Steam Technologies (IST) of Cambridge, Ontario was awarded the contract to provide the once-through steam generator. IST hired Airflow Sciences to perform Computational Fluid Dynamic (CFD) flow modeling and flow testing to aid in the design of the OTSG.

Full Story….

WPCA NEWS
Worldwide Pollution Control Association
www.wpca.info
A Bi-Annual News Journal Sponsored by the WPCA Winter - 2017

Executive Summary (cont.)

High Frequency TR Set (HFTR) Performance Comparison with Mid Frequency TR in Cement Plant Application

By Elavarasu Jayakumar, Stock Equipment

Schenck Process Solutions India Pvt Ltd (SPG) received an order to replace conventional TR set with high frequency TR set (HFTR) on Unit-8 of Shree Cements Limited (SCL) in RAS, Rajasthan. Prior, this facility installed one mid-frequency controller (MFTR) on Unit-3 with mixed results. This article will show the differences in operation and collection efficiencies between the MFTR and the HFTR.

Full Story….

Development of SCR Catalyst Regeneration Process for Enhanced Mercury Oxidation

By Thies Hoffmann, Xin Liu, Nick Pollack, Mike Mattes Cormetech Inc, Tobias Schwämmle and Thorsten Dux, STEAG Energy Services GmbH.

Mercury oxidation of OEM enhanced and regenerated catalyst samples were evaluated under a wide range of flue gas conditions the catalyst might be expected to perform. To address utility concerns regarding the regenerability of enhanced OEM Hg Oxidation catalysts, an optimized regeneration method was developed and demonstrated under lab conditions to meet OEM enhanced Hg Oxidation Catalyst performance levels.

Full Story….

Operating Challenges of Existing SCR and DSI Systems

By Suzette Puski, Babcock Power Inc.

With dispatch requirements resulting from changing generation portfolios, coal fired generating units are facing challenges running their SCR and DSI systems to meet emissions requirements. Maintaining flue gas and temperature distribution is important to maintain permitted emissions, maintain marketability of flyash and optimize O&M. The keys to addressing these challenges are a comprehensive understanding of the design and operation of the equipment and technology and expertise to apply solutions, such as static mixers, to resolve these issues

Full Story….

WPCA NEWS
www.wpca.info
A Bi-Annual *News Journal* Sponsored by the WPCA
Winter 2017

WORLDWIDE POLLUTION CONTROL ASSOCIATION

Consequences of Selenium Behavior in Coal-Fired Boilers on FGD Wastewater Treatment

Written by Connie Senior and Sharon Sjostrom, ADA-ES, Inc.

INTRODUCTION

Selenium is an essential micronutrient, but it can be toxic at higher doses. In the environment and in vivo the form of selenium is important: elemental selenium, metal selenides, and selenites have low solubility in water, but selenate ions are soluble and can affect the health of aquatic organisms.

Selenium air emissions from coal-fired electric utility boilers in the U.S. are regulated by the Environmental Protection Agency (EPA) under the Mercury and Air Toxics Standards (MATS) rule. Most plants meet the regulatory limit by controlling filterable particulate matter. In 2015, the EPA, under authority of the Clean Water Act, promulgated new Effluent Limitation Guidelines (ELG) for water discharges from steam electric power plants that specify effluent limits for arsenic, mercury, selenium, and nitrogen in wastewater discharged from wet scrubbers.[1] This rule was based on EPA's review of wastewater discharges from power plants and review of available treatment technologies.[2]

The ELG limit for selenium in FGD wastewater is 23 µg/L (ppb) for a daily maximum and 12 ppb for a 30-day average. Currently, the EPA is reviewing the ELG limits for FGD wastewater. It is possible that the limits may change in the future.

SELENIUM IN THE ENVIRONMENT

Selenium is a metal-like element, or metalloid, lying in the same column as sulfur in the periodic table. The chemistry of selenium bears similarity to that of sulfur. On a cellular level in biological systems, selenium is a component of certain proteins essential for cellular structure and defense against oxidative damage. Thus, selenium is an essential nutrient for animals (including humans) and some plants. However, selenium is toxic in higher concentrations. The transition between no observable effects and severe effects occurs over a narrow range of selenium concentrations.[3]

Selenium is found naturally in solids such as coal and organic-rich shales, which are utilized in a variety of

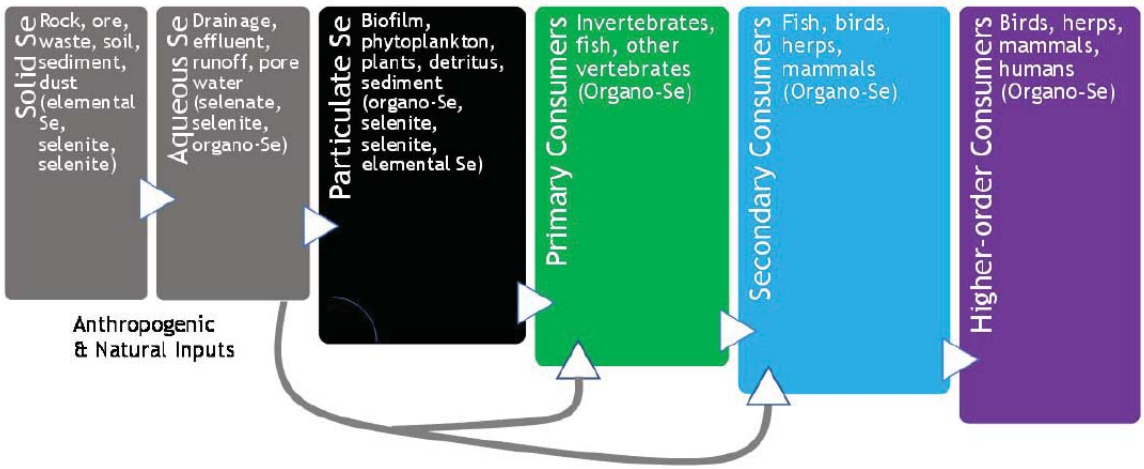

Figure 1: Selenium dynamics and transfer in aquatic ecosystems

industrial sectors (e.g., mining, oil refining, power generation). Discharges from agricultural and industrial activities can increase selenium concentrations in aquatic systems, in which toxicity is a concern.

Concern about the impact of selenium in aquatic ecosystems has been growing globally. The primary pathway for exposure to selenium for both invertebrates and vertebrates is diet (*Figure 1 on page 1*). Traditionally, exposure toxicity of a given substance in aquatic systems is predicted based on dissolved concentrations. However, these methods don't work well for selenium compounds, because the behavior and toxicity of selenium in aquatic systems are dependent on factors such as the structure of the food web and hydrology, which are site-specific.

As with other trace contaminants such as mercury, bioaccumulation of selenium occurs across food webs. Selenium uptake is promoted across most biological membranes, which makes its partitioning unique among metalloid contaminants. Another differentiator for selenium is the narrow range between essential dietary requirements and toxicity.

Selenium toxicity is exhibited primarily as reproductive impairment, for example, embryotoxicity or mutations in egg-laying vertebrates. Mammals in aquatic food webs do not appear to be as sensitive to dietary exposure to organic selenium compounds as fish or birds. The most sensitive toxicity endpoint for birds, is embryo mortality, while for fish larvae, a range of severe developmental abnormalities have been catalogued.[3]

Risk assessment of selenium exposure must be site-specific to a much greater extent than other contaminants. Furthermore, a single, universal dissolved water quality value is not adequate for predicting toxicity across a range of sites. Concentrations of selenium in fish and bird eggs at a given location are critical to assessing risk, because concentrations in these tissues are most strongly linked to adverse effects.

In the U.S., increases in selenium concentration in reservoirs have provided examples of the impact of selenium on aquatic life. For example, Belews Lake in North Carolina experienced high influxes of selenium from the nearby power plant, which discharged the overflow from ponds contained sluiced fly ash and bottom ash into the lake from 1974 to 1985. Selenium concentrations in the ash pond discharge water were high (150–200 µg Se/L) according to Lemly.[5] Deformities and reproductive failure in the fish population decimated nineteen of twenty species of fish in the lake. In 1986, the discharges were eliminated to the lake and fish populations recovered. Selenium concentrations in the lake's biota were reduced by 85-95% after ten years, although elevated selenium concentrations in the sediments still posed a risk to fish.[6]

SELENIUM BEHAVIOR IN COAL-FIRED BOILERS

Selenium is found in coals in trace concentrations. A typical range of concentrations in U.S. coals is 0.5 to 10 µg/g.[7] The mode of occurrence of selenium in coal has been investigated using selective leaching (chemical fractionation). The predominant modes of occurrence are association with pyrite and association with the organic matter. Minor amounts of selenium are sometimes associated with HCl-soluble sulfides and silicates.[8] The minerals in bituminous coals from the Eastern U.S. can contain significant amounts of pyrite, and selenium in those coals is often mostly associated with pyrite. In subbituminous coals from the Powder River Basin (PRB), selenium is mostly associated with the organic matrix.

The behavior of selenium during combustion and in air pollution control devices is different from other trace metals because of the high vapor pressure of the oxide (SeO_2). Selenium can exist in the gas phase (as SeO_2) at temperatures above 160°F in coal-fired power plants.[9] In the boiler, gaseous SeO_2 can be chemisorbed on the fly ash surface (even at temperatures in the furnace convective section),[10] but some selenium can remain in the vapor phase at the exit of the particulate control device. Selenium has been shown to react with both calcium and iron compounds in the fly ash from coal combustion.[11] The presence of SO_2 in the flue gas interferes with the reaction between SeO_2 and fly ash. In boilers burning low-sulfur western coals with high concentrations of calcium in the fly ash, most of the selenium is converted to the particulate phase in the flue gas. In contrast, in boilers burning high-sulfur bituminous coal, considerably less selenium is converted to the particulate phase in the flue gas. Most of the particulate-bound Se is removed in the particulate collection device. The remaining Se enters the wet FGD scrubber as vapor-phase or residual particulate-phase selenium.

Wet scrubbers typically have greater than 98% SO_2 removal and 95% $HgCl_2$ removal[12], but the limited data indicate less removal of SeO_2. This discrepancy is not due to concentration-dependent gas-phase mass transfer, as SeO_2 is present in significantly higher amounts than $HgCl_2$ and significantly lower amounts than SO_2. This discrepancy is also not due to

solubility, because SeO_2 is the most soluble of the three species. One theory is that, since the flue gas enters the scrubber at a temperature of 275°F to 375°F, and then undergoes a rapid quench to a temperature in the range of 120°F to 130°F, there may be sufficient driving force to condense H_2SeO_3, either heterogeneously (on submicron ash particles) or homogeneously. Since submicron particles are not efficiently captured by wet scrubbers, this could explain the lower than expected removal of selenium across wet FGD scrubber. An alternate hypothesis is that droplets of scrubber slurry are entrained in the flue gas; the droplets contain selenium in the solid phase, which is carried out of the scrubber as particulate selenium.[18]

One study at full-scale on a 900 MW coal-fired power plant with electrostatic precipitator (ESP) and wet flue gas desulfurization (FGD) scrubber appeared to confirm the former theory.[13] Results from the study showed that there was a significant fraction of selenium entering the scrubber that was not captured by the scrubber.[13] Based on the observed size-dependence of selenium concentration in the exiting fly ash in this study, gaseous selenium appeared to condense on particles across the scrubber, which were not efficiently captured.

Limited data sets exist on selenium in the flue gas of full-scale power plants. Selected published data[13-17] are summarized in *Figure 2*. The coal-fired boilers included either had cold-side electrostatic precipitators (ESPs) or fabric filters (FFs). All units had wet FGDs. Several boilers had a selective catalytic reduction (SCR) unit for NOx control; one boiler had a selective non-catalytic reduction (SNCR) unit for NOx control. Removal of Se across the ESPs varied from 32% to 82% (bituminous units); removal across the FFs varied from 52% to 72% (low-rank units). Removal of Se across the FGDs was in the range of 53% to 96%.

IMPLICATIONS FOR WASTEWATER TREATMENT

Once selenium from the flue gas has been captured by a wet FGD system, understanding the fate of selenium in the scrubber is critical in the light of the limits imposed by the Effluent Limitation Guidelines on the discharge of selenium in FGD wastewater. Selenium that is captured by the scrubber can end up in the gypsum or scrubber byproduct or in the wastewater (the blowdown or chloride purge stream).

The disposition of selenium in wet FGD scrubber is highly variable and influenced by the design and operation of the scrubber. In one study encompassing eight boilers with scrubbers,[17] the percentage of boiler input selenium accounted for in the byproduct gypsum ranged from 13 to 20% in the bituminous coal-fired units, while the chloride purge streams accounted for 2 to 5%. In contrast, in the subbituminous coal-fired units only 1 to 9% of the boiler input selenium was accounted for in the gypsum and 0 to 2% was accounted for in the chloride purge streams. In another study of two coal-fired boilers,[18] at one boiler, 10% of the boiler input selenium left the scrubber in the gypsum, and 2% in the

Plant	Coal	MW	NOx Ctrl	PCD	DSI	SO_2 Ctrl	PCD Removal	FGD Removal
900 MW[13]	Bituminous	900	--	ESP	Yes	wet FGD	--	61%
Yates[14]	Bituminous	100	None	ESP	No	wet FGD	49%	66%
US1[15]	Bituminous	795	SCR	ESP	No	wet FGD	61%	90%
ES1[16]	Subbit.	--	None	ESP	No	wet FGD	38%	62%
Plant B1[17]	Bituminous	207.9	SCR	ESP	No	wet FGD	35%	86%
Plant B2[17]	Bituminous	203.2	SCR	ESP	No	wet FGD	84%	75%
Boiler C[17]	Bituminous	175	SCR	FF	No	wet FGD	25%	96%
Plant D1[17]	Bit./Petcoke	150.7	SCR	ESP	No	wet FGD	41%	53%
Plant D2[17]	Bit./Petcoke	260.7	SNCR	ESP	No	wet FGD	32%	53%
Boiler F[17]	Subbit.	566	--	FF	No	wet FGD	52%	57%
Plant G1[17]	Subbit.	448.5	--	FF	No	wet FGD	72%	83%
Plant G2[17]	Subbit.	440	--	FF	No	wet FGD	70%	79%

Figure 2: Selenium removal across particulate control devices (PCDs) and FGDs at coal-fired power plants

FGD water discharge. At the other boiler in this study, 4-9% of the boiler input selenium left the scrubber in the gypsum, while 6-21% was in the FGD water discharge.

It is instructive to compare the current ELG limits for selenium in FGD water discharge with what is observed in full-scale FGDs. A survey of operating conditions and metals in FGD scrubbers from 18 coal-fired boilers, featuring a range of different coal types and two different scrubber types, was summarized by Allen et al.[19] Average selenium concentrations in scrubber slurries varied from 100 µg/L to 10,000 µg/L. Selenium that leaves the scrubber in the wastewater discharge may have to be treated to reduce the concentration to meet the current daily maximum ELG limits of 23 µg/L.

Further complicating the picture, different species of selenium have been observed in FGD slurries. Highly oxidizing conditions in the scrubber slurry promote the formation of oxidizing species, like dithionate and peroxydisulfate,[20] which result in the presence of mostly selenate (Se[VI]) in the scrubber liquor. Selenate is not removed by traditional physical/chemical wastewater treatment systems. If there are high concentrations of selenate in the scrubber wastewater discharge, an additional treatment step like a biological reactor will be required.

In the study by Allen et al., the total selenium concentrations in the scrubber slurries were not correlated with oxidation-reduction potential (ORP) in the slurry, but the fraction of dissolved selenium and the speciation of the dissolved selenium was correlated with ORP. The fraction of dissolved selenium was generally less than 50% for ORP values less than 350 mV. Below 400 mV ORP, selenite was the major selenium species in the dissolved fraction. For ORP values above 400 mV, almost all the dissolved selenium was selenate.[19] In another study, samples collected from full-scale LSFO systems also showed a similar effect of ORP on the fraction of dissolved selenium as selenite.[21]

Results of bench-scale testing[21] showed that low ORP (150-200 mV) and low pH favored selenite formation. ORP had a larger effect on selenium speciation than pH. Reducing oxidation air (and hence ORP) was shown to be a strategy for shifting dissolved selenium to selenite and for reducing the fraction of dissolved selenium in the scrubber slurry. Other factors affected speciation: for example, solid manganese oxides promoted formation of selenite, but dissolved Mn[II] did not oxidize selenite to selenite.

Pilot-scale tests were carried out at a power plant in which FGD slurry for the pilot-scale system was drawn from the host unit's FGD scrubber.[22] The host unit FGD operated at high ORP (~ 600 mV). Forty to forty-five percent of the selenium was in the dissolved phase, and all the selenium in the dissolved phase was found as selenate. Testing in the pilot-scale unit did not have much success in reducing the ORP below 400 mV. The pilot scrubber also had a hydroclone, which is commonly used to separate the gypsum or solid byproduct from the aqueous part of the slurry. Most of the solid selenium (70-86%) reported to the hydroclone underflow stream (i.e., gypsum product), while less solid selenium was found in the fines. For mercury, on the other hand, the fates of solid phase mercury were reversed: most of the solid phase mercury reported to the fines.

If metal concentrations in the chloride purge stream are high enough to be of concern, wastewater treatment (WWT) might be required prior to discharging any FGD wastewater. While every FGD scrubber will be different, owing to different coal compositions being fired and differences in operation, the observations discussed above point to general regimes of operation as illustrated qualitatively in *Figure 3*. Scrubber ORP provides guidance on the effectiveness of different post-FGD treatment processes for selenium. Dissolved selenite and particulate-phase selenium can be removed in a physical-chemical WWT process. However, dissolved selenate cannot be removed in physical-chemical treatment

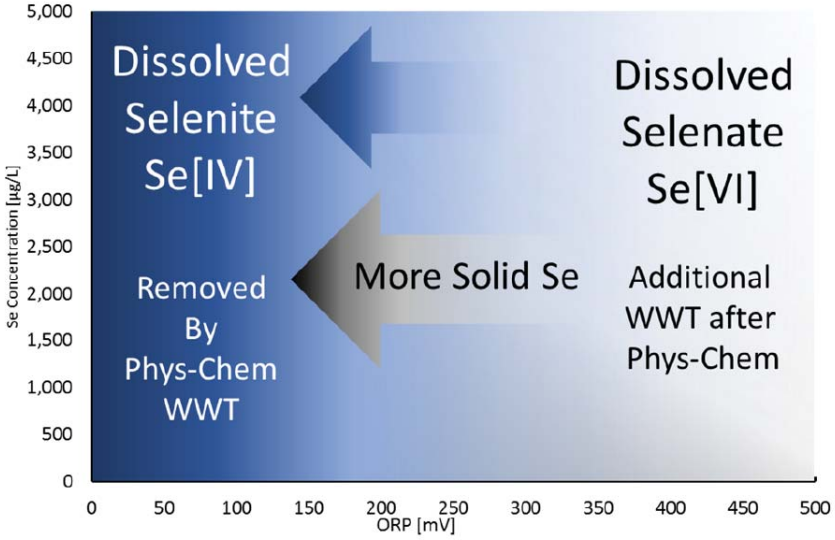

Figure 3: Selenium speciation and partitioning in scrubber slurries

process. Additional treatment after a physical-chemical process might be required to reduce concentrations of selenate to acceptable levels. Biological reactors are the most mature technology for selenate reduction, although other processes are under development and being tested at pilot scale.

In some plants, the hydroclone overflow stream is recirculated back to the scrubber. Recirculation of the filtered water (i.e., the hydroclone overflow stream) has been shown in full-scale scrubber studies to result in high concentrations of selenium (and other metals) in the scrubber slurry. [18] It is possible that, as the concentration of selenium cycles up in the slurry, the more of the recirculated selenium reports to the gypsum product.

There are many trade-offs in operating the scrubber as well as the upstream air pollution control equipment to meet limits on selenium concentrations in FGD wastewater discharge. A few of the trade-offs are:

- Upstream removal of selenium before the FGD;
- Minimization of blowdown/chloride purge stream;
- Concentration of selenium in recirculated water;
- Solid-liquid partitioning in the scrubber slurry.

These factors are by no means comprehensive, but they do represent some of the means that scrubber operators could affect the amount and species of selenium entering the wastewater treatment system. Note that every combination of fuel and scrubber will yield different outcomes.

CONCLUSIONS

There are many factors that affect the amount of selenium that is captured in a wet scrubber and the amount of selenium leaving the scrubber in the chloride purge stream. The concentrations and speciation of selenium in the chloride purge stream affect the cost and complexity of the waste water treatment system. Selenite in the dissolved phase and, presumably, selenium solids in the fines could be treated in a conventional physical-chemical wastewater treatment process. However, selenate in the dissolved phase would require an additional treatment step. Biological treatment is currently the process recommended for removing selenate, although other technologies are under development.

In terms of methods for control, there may be an optimal point where ORP can be minimized in a limestone forced oxidation scrubber to keep most of the selenium as selenite. Other factors such as dissolved transition metals and scrubber additives will also affect selenium speciation and liquid-solid partitioning. While some FGD systems might be able to control the formation of selenate by control or ORP, this is by no means a universal conclusion; some FGDs might have to operate at higher ORP values to maintain acceptable levels of sulfite in the gypsum product. A high level of selenium removal upstream of the FGD will reduce the selenium concentration in the scrubber and chloride purge stream, although it will not address the important question of selenium speciation in the scrubber.

Other aspects of scrubber operation should be considered as to their impact on selenium in the chloride purge and in the gypsum product. Cycling up the scrubber reduces the amount of water to be treated in a wastewater treatment system, but increases the absolute concentration of selenium in that stream. Using recirculated water for scrubber make-up water can have an impact on selenium in the scrubber and should be considered.

Operating a coal-fired power plant requires a systems view, considering multiple factors including regulatory limits at the stack and effluent pipe, byproduct quality, fuel purchase economics, overall plant operations and maintenance. Adding selenium chemistry to the mix of factors to consider further complicates operations and increases the importance of incorporating a systems perspective.

REFERENCES

1. *40 CFR Part 423, Effluent Limitations Guidelines and Standards for the Steam Electric Power Generating Point Source Category; Final Rule; U.S. Environmental Protection Agency, Code of Federal Regulations Vol. 80, No. 212, November 3, 2015.*
2. *Steam Electric Power Generating Point Source Category: Final Detailed Study Report. EPA 821-R-09-008; U.S. Environmental Protection Agency, U.S. Government Printing Office: Washington, DC, 2009.*
3. *Hamilton, S.J. Review of selenium toxicity in aquatic food chains. Sci. Total. Env. 2004, 326, 1-31.*
4. *Chapman, P.M., et al. Ecological Assessment of Selenium in the Aquatic Environment: Summary of a SETAC Pellston Workshop. Pensacola, FL, February 22-28, 2009.*
5. *Lemly, A.D. Ecosystem Recovery Following Selenium Contamination in a Freshwater Reservoir. Ecotoxicology 1997, 36, 275-281.*
6. *Lemly, A.D. Selenium Assessment in Aquatic Ecosystems. Springer, 2009. pp 39-58.*
7. *Akers, D.J., et al. HAPs-Rx : Precombustion Removal of Hazardous Air Pollutant Precursors. Final Report DOE Contract No. DE-AC22-95PC95153, March, 1998.*
8. *Palmer, C.A.; Mroczkowski, S.J.; Finkelman, R.B.; Crowley, S.S.; Bullock, J.H. The use of sequential leaching to quantify the modes of occurrence of elements in coal. Proceedings of 15th Annual Pittsburgh Coal Conference, Pittsburgh, PA, September 15-17, 1998.*
9. *Martin, C.; Pavlish, J.; Zhuang, Y. Impacts of Condensation on Selenium Transport and Capture. In Proceedings of Air Quality VIII, Arlington, VA, October 23-27, 2011; Energy & Environmental Research Center: Grand Forks, North Dakota, 2011.*
10. *Senior, C.; Van Otten, B.; Wendt, J.O.L.; Sarofim, A. Modeling the*

behavior of selenium in pulverized-coal combustion systems. Combust. Flame 2010, 157, 2095-2105.

11. *Seames, W.S.; Wendt, J.O.L. Regimes of association of arsenic and selenium during pulverized coal combustion. Proc. Comb. Inst. 2007, 31, 2839-2846.*
12. *Senior, C.L. Review of the Role of Aqueous Chemistry in Mercury Removal by Acid Gas Scrubbers on Incinerator Systems. Environ. Eng. Sci. 2007, 24, 1128-1133.*
13. *Senior, C.L.; Tyree, C.A.; Meeks, N.D.; Acharya, C.; McCain, J.D.; Cushing, K.M. Selenium Partitioning and Removal Across a Wet FGD Scrubber at a Coal-Fired Power Plant. Env. Sci. Technol. 2015, 49, 14376-14382.*
14. *Burns and Roe Services Corporation, Summary of Air Toxics Emissions Testing at Sixteen Utility Power Plants, Report for US DOE Contract DE-AC22-94PC92100, July 1996.*
15. *Cheng, C.-M.; Hack, P.; Chu, P.; Chang, Y.-N.; Lin, T.-Y.; Ko, C.-S.; Chiang, P.-H.; He, C.-C.; Lai, Y.-M.; Pan, W.-P. Energy Fuels 2009, 23, 4805-4816.*
16. *Álvarez-Ayuso, E.; Querol, X.; Tomás, A. Chemosphere 2006, 65, 2009-2017.*
17. *Senior, C.; Blythe, G.; Chu, P. Multi-Media Emissions of Selenium from Coal-Fired Electric Utility Boilers. Presented at Air Quality VIII, Arlington, VA, October 23-27, 2011.*
18. *Córdoba, P. Partitioning and speciation of trace elements at two coal-fired power plants equipped with a wet limestone Flue Gas Desulphurisation (FGD) system. PhD Thesis, Universitat Politènica de Catalunya, 2013.*
19. *Allen, J.O.; Ferens-Foulet, C.K.; Acharya, CK. Effluent Trace Metals Survey and Related Plant Operations at 18 Flagship Units. Presented at Power Plant Pollutant Control and Carbon Management "Mega" Symposium, Baltimore, MD, August 16-19, 2016.*
20. *Gutberlet, H.; Boehm, G.M. The Influence of Induced Oxidation on the Operation of Wet FGD Systems. Presented at the Air Quality V Conference, September 19-21, 2005, Arlington, VA.*
21. *Blythe, G.M.; Richardson, M.K.; Chu, P.; Dene, C.; Wallschlager, D.; Searcy, K.; Fisher, K. Selenium Speciation and Partitioning in Wet FGD Systems. Presented at Power Plant Air Pollution Mega Symposium, Baltimore, MD, August 30-September 2, 2010.*
22. *Searcy, K.; Richardson, M.; Blythe, G.M.; Wallschlager, D.; Chu, P.; Dene, C. Selenium Speciation and Management in Wet FGD Systems. Final Report DE-FG02-08ER84948, 2012.*

For further information, contact
Connie Senior at connies@adaes.com

BIOGRAPHY

Dr. Connie Senior is Vice President of Technology at ADA-ES, Inc. She is an internationally recognized expert on mercury control from coal-fired boilers. She serves on EPA's Board of Scientific Counselors. She has worked on understanding and predicting the behavior of mercury and other hazardous air pollutants for over fifteen years and has more than ten years' experience with demonstrations of full-scale mercury emissions control.

Sharon Sjostrom is the Chief Product Officer at Advanced Emissions Solutions, Inc. where she is responsible for leading strategic product and business development for the corporation through its subsidiary ADA-ES, Inc. Sharon has over 25 years of experience developing technologies and commercializing products that reduce emissions from coal-fired power generation, with a focus on mercury controls. She has published more than fifty technical papers and is an inventor on sixteen patents.

ADA
Advancing Cleaner Energy

Wet Electrostatic Precipitator Application for Coal-fired Boiler

Written by Hardik Shah, Southern Environmental, Inc

Wet Electrostatic Precipitators (WESPs) are used to capture sub-micron particulate in a wide range of industrial applications. WESPs are usually installed downstream of a saturator or a wet scrubber and typically used as a particulate and mist "polishing" device. Although WESPs are a proven technology for sub-micron particulate and acid mist capture, a major O&M issue is performance degradation due to material build-up on collecting electrodes which results in close electrode clearances and decreased corona voltage and current. It is time consuming and expensive to remove build-ups and repair close clearances, and this task often must be performed during short process turn-arounds. And when it becomes necessary to replace an entire set of collecting electrodes, this task typically involves removing the roof of the WESP and hiring specialized skilled laborers to perform the work. This results in both longer turn-around durations and higher O&M costs.

In order to address this problem SEI has developed an innovative design in which fabric membranes replace the lead, exotic metal or plastic collecting electrodes typically used in a WESP. Fabric membranes are hung in a similar manner as with any other collecting electrode, but are continuously irrigated with liquid to keep them clean and electrically conductive. Membrane material is typically polypropylene which is readily available and has excellent chemical resistance properties in a low pH environment.

One common WESP application is to install it downstream of a wet scrubber on a coal-fired boiler in order to capture fine particulate. One Midwestern USA industrial facility recently installed a Southern Environmental, Inc. (SEI) innovative WESP in which the collecting electrodes are fabricated from felted polypropylene. This WESP design was selected by the end user based upon both low capital cost and mitigation of O&M issues.

This industrial facility has a stoker-fired boiler with air pollution control equipment arranged as shown in *Figure 4*. In order to comply with the industrial boiler MACT particulate matter emission limit of 0.04 lb/mmBtu, this facility considered various technology options as shown in *Figure 5* on page 8.

After careful evaluation the end user selected SEI's WESP technology as it was concluded to be both technically superior and the most economical option.

The boiler fires an Eastern Kentucky coal with moderate sulfur content (1% typical) and moderate ash content (6.0 to 6.6%). The WESP's design conditions and the results of SEI's performance guarantee test are listed in *Figure 6* on page 9.

Due to the highly corrosive nature of the application, all metal parts contacting the gas stream in this WESP were fabricated from Duplex 2205 SS. The collecting electrodes were made out of felted polypropylene. Duplex 2205 SS was carefully selected considering the operating pH and chloride concentration. It should be noted that the chloride concentration in this application is considerably lower than what is typically found in Wet FGD application in coal-fired power plants. After two years of operation, no noticeable corrosion has been observed in this unit.

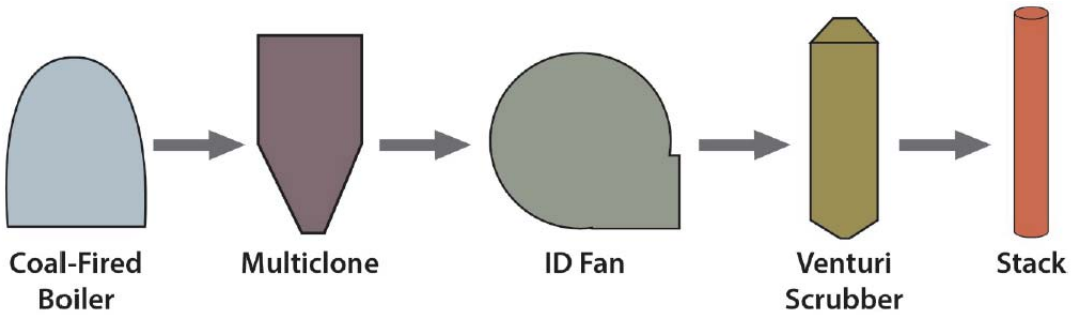

Figure 4: Existing Arrangement

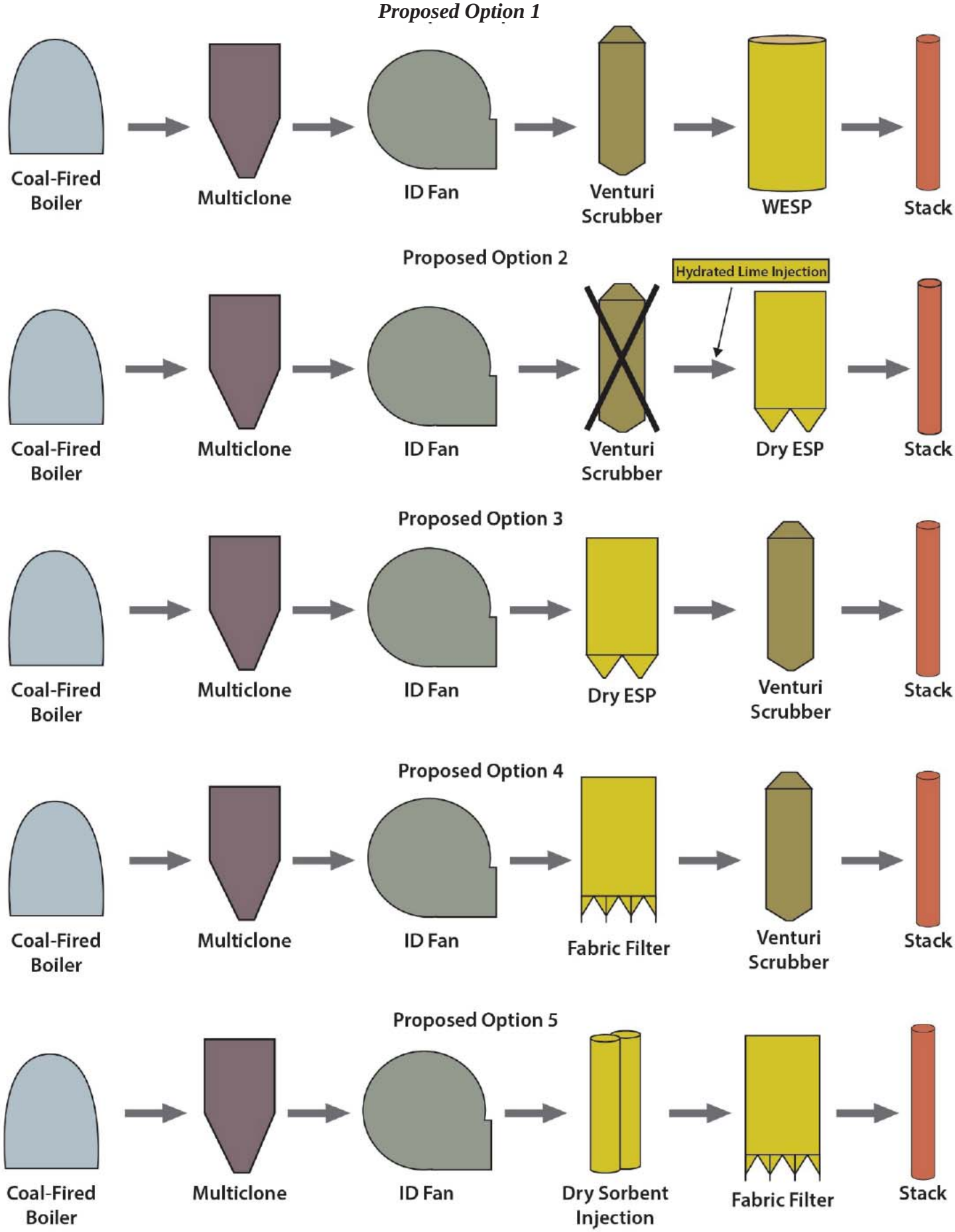

Figure 5: Proposed Option 1

	Design Conditions	Performance Test, Oct-15
Saturated Gas Flow Rate, acfm	81,133	71,679
Saturated Temperature (deg F)	140	125
Inlet PM Loading (lb/mmBtu)	0.176	0.1
Stack PM Emissions (lb/mmBtu)	0.04	0.0195
Removal PM Efficiency (%)	77.27%	80.50%

Figure 6

SEI's membrane WESP is a tubular, up-flow design consisting of a single module as shown in the photograph on page 9: *Figure 7* .

As shown in *Figure 8* on page 10, this module consists of a single mechanical field but two independent, parallel electrical bus-sections. By having two independent parallel bus-sections, one half of the WESP module is always in operation while the other half is periodically washed. This provides added reliability and redundancy to the system without adding significant capital cost.

A major advantage of SEI's WESP technology is the maintenance friendliness of its fabric membrane collecting electrodes. The membrane material is typically purchased in rolls which allows for easy entry and exit through WESP access doors. Once the membranes are in place and the WESP is returned to operation, any close clearance problems that may develop between membranes and discharge electrodes can be easily resolved by replacing individual membrane pieces. If replacement proves infeasible, the affected membrane section can be easily removed using a scissors or knife. When it is necessary to replace an entire set of collecting electrodes all work can be performed without having to remove the WESP's roof. The replacement of membrane type collecting electrodes for this coal-fired boiler WESP installation can be done in one week.

In the past twelve years SEI's membrane WESP design has been applied to many applications such as oil-fired boilers, fiberglass insulation forming lines, the gas cleaning system of an acid plant, and coal-fired boilers. Membrane collecting electrodes have demonstrated several years of life under typical WESP operating temperatures and with measured pH's as low as 0.5.

Figure 7 (below)

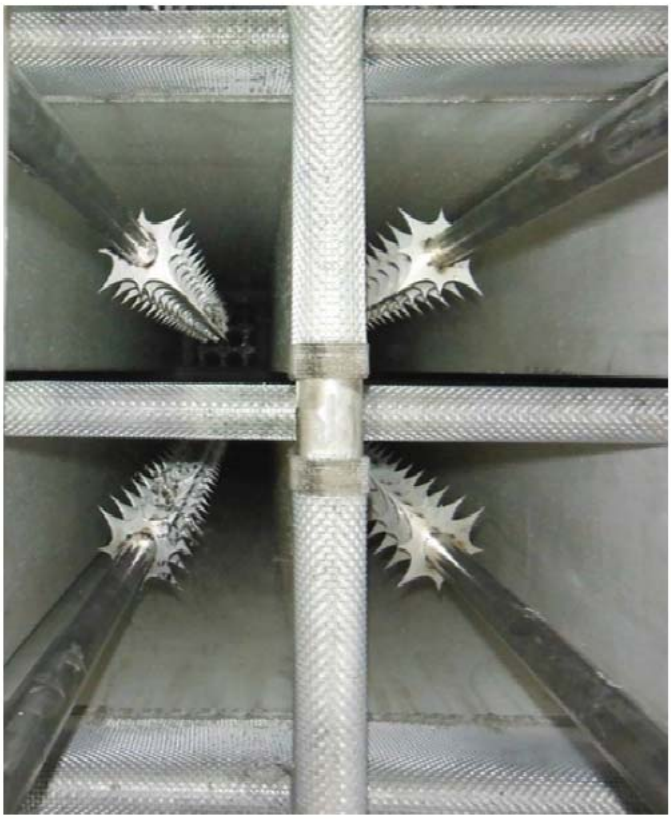

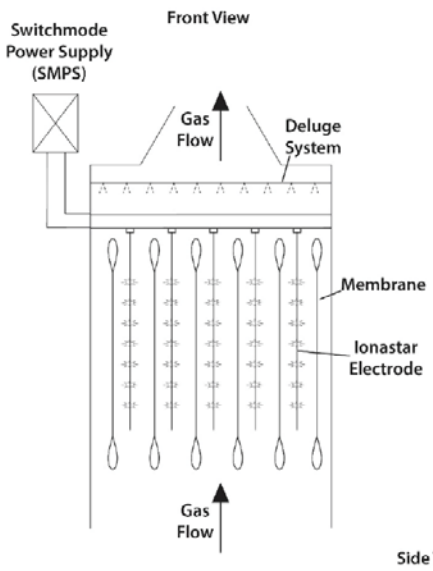

Figure 8

For further information contact Hardik Shah at hshah@sei-group.com

BIOGRAPHY

Hardik Shah of Southern Environmental, Inc. has more than 12 years of experience in the air pollution control industry. His primary area of focus is applications work with Dry and Wet Electrostatic Precipitators. Hardik holds a B.E degree in Mechanical Engineering from M.S. University, India and M.S. degree in Mechanical Engineering from Ohio University

WPCA NEWS
www.wpca.info
A Bi-Annual Newsletter Sponsored by the WPCA

Is a bi-annual technical journal sponsored by and for the Worldwide Pollution Control Association
www.wpca.info

Purpose

To foster new ideas and greater awareness concerning pollution control in the energy industry

Publisher

Reinhold Environmental Ltd.

Comments & Other Inquiries to:

Reinhold Environmental
3850 Bordeaux Drive
Northbrook, IL 60062 USA
1.847.291.7396
sreinhold@reinholdenvironmental.com

For more information on the WPCA Please visit our website at
www.wpca.info

Limitations in Reduced Load SCR Operation

Written by Joakim Reimer Thøgersen, Ph.D., Chem. Eng., Vice President, R&D,
Hans Jensen-Holm. Ph.D., Chem. Eng., General Manager, Technical Support
Haldor Topsøe A/S, Nymøllevej 55, DK-2800 Kgs. Lyngby

INTRODUCTION

As the wind-turbine capacity has been increased in Denmark the need to operate thermal power plants at reduced load has increased. At the same time a domestic NOx tax of 3.4 Euro per kg NOx gives an incentive to remove as much NOx as possible. Increased wind-power capacity and tightened NOx regulations are an expected trend in the rest of Europe and the U.S. in the years to come. There is therefore an increased focus on operation of the SCR DeNOx units at lower loads.

Optimization strategies for SCR units operating at reduced load include the standard measures such as ammonia, temperature and flow distribution and installation of additional catalyst layers. In some cases it is also an option to split the boiler economizer in order to increase the SCR temperature. However, this is an expensive solution, and an economically attractive solution is to implement an ammonia-injection strategy.

In boilers fired with sulfur-rich fuels, the minimum operating temperature in SCR DeNOx is determined by the dew point of ammonium salts. At reduced boiler load it becomes critical to have accurate predictions of the dew point. Experimental simulations of a coal-fired SCR installation and an oil-fired installation have confirmed previously determined dew-point correlations [1] for formation of ammonium salts. Due to capillary forces in the catalyst an effect of ammonium bisulphate, ABS, condensation is seen from approximately 28°C above the bulk gas phase dew point and the inhibition is reversible by thermal treatment. A new finding is a hysteresis effect, meaning that regeneration up to a certain inhibition level requires a somewhat higher temperature than the temperature at which this level is reached when the temperature is decreased from above the ABS dew point. A predictive ABS-inhibition model developed at Haldor Topsøe satisfactorily describes the equilibrium inhibition levels and the dynamic behavior of ABS inhibition. Flue gas data on power plant operation around the ABS dew point in the SCR is now available and these data show that optimization of SCR performance at reduced load is possible.

Haldor Topsøe's DNX® catalyst with its high porosity ensures optimal resistance against ABS condensation and combined with the Haldor Topsøe design tools, SCR DeNOx operation around the ABS dew point can be utilized to the maximum possible extent.

AMMONIUM BISULPHATE DEWPOINT AND SCR DENOX PERFORMANCE

The minimum process temperature in SCR DeNOx with ammonia injection is determined by formation of ammonium salts. The injected NOx reducing agent, ammonia, reacts with the acid gases in the flue gas forming ammonia salts, i.e. ammonium chloride, NH_4Cl, ammonium bisulphate, NH_4HSO_4, and ammonium nitrate, $(NH_4)_2NO_3$. In most cases NH_4HSO_4 has the highest dew point, but in waste incineration units with HCl concentrations of several hundred ppm, NH_4Cl condensation determines the minimum temperature. In chlorine- and sulfur-free flue gases the minimum temperature is determined by the $(NH_4)_2NO_3$ dew point. SCR installations in coal-fired power plants are normally operated at temperatures between 330°C and 430°C with ABS catalyst dew points typically between 280°C and 320°C. Below the dew point ammonia and sulfuric acid condense as liquid ammonium bisulphate, NH_4HSO_4, in the catalyst pore structure which inhibits the performance. The bimolecular condensation reaction is written as:

$$NH_{3(g)} + H_2SO_{4(g)} \rightarrow NH_4HSO_{4(l)}$$

At SCR DeNOx temperatures gaseous sulfuric acid is in equilibrium with SO_3 and the ABS dew point therefore depends on the water content, ammonia content and SO_3 concentration:

$$SO_3 + H_2O \rightarrow H_2SO_4$$

Ammonium bisulphate has a melting point of 147°C. Formation of ammonium sulphate $(NH_4)_2SO_4$ is thermodynamically more favorable but analysis of condensed salts has shown that $(NH_4)_2SO_4$ is only formed in limited amounts due to kinetic limitations [2,3].

ABS inhibition of the catalyst is reversible and ABS is readily evaporated by raising the catalyst temperature. The bulk dew point in the SCR reactor inlet is typically around 290°C but the observed dew point is higher due to capillary forces in the micro pore structure. The ABS dew point decreases through the SCR reactor since NH_3 is consumed in the SCR reaction. According to Matsuda [1] the bulk dew point is as a good approximation given by the Clausius-Clapeyron equation:

$$\ln\left(P_{NH_3}\cdot P_{H_2SO_4}\right)_{eq,bulk} = 27.97 - \frac{26671}{T[K]}$$

where P_i [atm] are partial pressures in the gas phase. The influence of the capillary forces is given by the Kelvin equation:

$$\ln\frac{\left(P_{NH_3}\cdot P_{H_2SO_4}\right)_{eq,pore}}{\left(P_{NH_3}\cdot P_{H_2SO_4}\right)_{eq,bulk}} = -\frac{2\cdot\sigma\cdot M}{\rho\cdot r_{pore}\cdot R\cdot T}$$

where r_{pore} is the pore size that is just filled with ABS at a given gas composition and temperature and s is the surface tension of ABS. Other sources [2,3] have reported dew points that are significantly lower compared to the Matsuda numbers. These numbers are based on observations of ammonium bisulphate and ammonium sulfate fouling of heat exchange surfaces. Depending on the process parameters such as gas velocity, gas passing area, gas temperature, metal temperature and particle concentrations a major part of the ammonium bisulphate formed will pass through the heat exchanger as aerosols. Another factor is super cooling. Both capillary condensation and super cooling are the results of a relatively high surface energy or surface tension of the condensing phase. These factors may result in lower observed dew points that are more relevant to heat exchanger surfaces. As a comparison the Clausius-Clapeyron equation derived from the data generated by Ando et al. [3] becomes:

$$\ln\left(P_{NH_3}[atm]\cdot P_{H_2SO_4}[atm]\right)_{eq,bulk} = 41.6 - \frac{30900}{T[K]}$$

The catalyst activity is directly related to the extent of pore condensation which means that ABS inhibition increases gradually as the temperature is lowered towards the bulk dew point. Model predictions show that 10 ppm SO_3' (SO_3 + H_2SO_4), 200 ppm NH_3 and 8% H_2O condense as ABS in pores smaller than approximately 38 Å at 317˚C. Operation below the bulk dew point is not an option except for very low SO_3 concentrations in a low dust SCR installation since ABS will condense not only inside the catalyst pores but also at the catalyst surface creating a sticky surface which could over time lead to pluggage of the catalyst.

The equation from Matsuda et al. [1] is very accurate in the prediction of the bulk dew point. The bulk dew point has been determined experimentally in the laboratory by identifying the temperature point where total catalyst inhibition is obtained. An overview of bulk dew point predictions and experimental observations are shown in *Figure 9*.

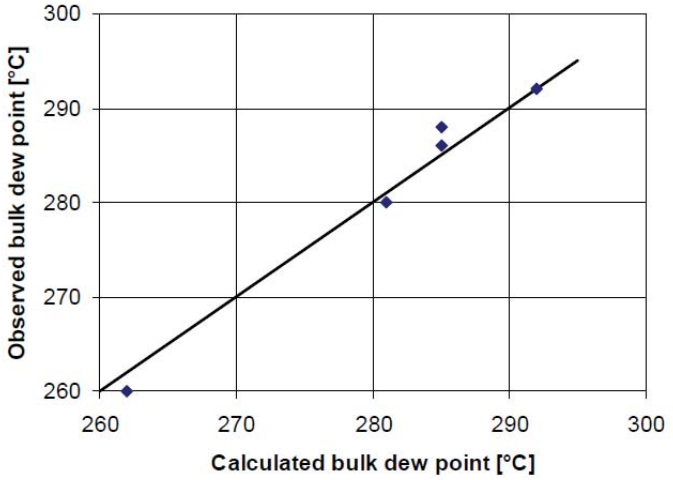

Figure 9: Relation between predicted and observed bulk dew points calculated according to Matsuda et al

A thermo-gravimetric analysis (TGA) of an SCR DeNOx catalyst sample with ABS in the pore structure shows the characteristics of ABS. The catalyst sample was operated below the ABS dew point until steady state was achieved. Then SO_3, ammonia and water dosing was stopped instantaneously and the sample was quenched in air. Subsequent TGA analysis of the catalyst sample revealed the following characteristics about ABS: Below 100°C water physisorbed during cooling and handling of the sample is released. ABS is hygroscopic at lower temperatures and chemisorbed water evaporates between 160°C and 210°C. Above 310°C ABS evaporates as NH_3, SO_3 and water from the sample. The physical behavior in the TGA analysis is a bit different from real SCR DeNOx flue gas conditions in that the inlet gas does not contain sulfur trioxide, ammonia and water. Some of the ABS is released at temperatures well above the dew point since the time is too short at the lower temperatures to regenerate the catalyst completely.

LABORATORY EXPERIMENTS

Laboratory reactor experiments have been carried out with process conditions that correspond to a typical oil-fired boiler operating case and a typical coal-fired boiler operating case, using a Topsøe low-dust type catalyst, DNX-LD, and a high-dust type catalyst, DNX-HD, respectively. The labora-

tory reactor is an isothermal reactor with compensation for heat loss. The reactor cross section has dimensions of 45 mm × 45 mm. 500-mm monolith catalyst was loaded in the reactor. The catalyst height is larger in a typical full scale installation and the experiments therefore show the behavior in the first part of a typical catalyst installation. The test conditions are listed in *Figure 10.*

		Coal fired boiler	Oil fired boiler
DNX type		HD	LD
NOx	[ppm]	300	150
NH_3/NO_x		0.9	0.8
Catalyst sample length	[m]	0.5	0.5
SO_2	[ppm]	3000	300
SO_3	[ppm]	30	3
O_2	[%]	3	1
H_2O	[%]	8	12
v_0	[Nm/s]	2	2
$T_{design\ dew\ point}$	[°C]	317	287
$T_{bulk\ dew\ point}$	[°C]	292	262

Figure 10: Experimental Conditions

v_0 denotes the linear gas velocity in the (empty) reactor and NH_3/NOx is the ammonia-to-NOx ratio in the feed gas. The design dew point is the temperature at which a typical installed catalyst volume in full scale (NHSV = 4000 h^{-1}) has approximately 95% residual activity.

The activity relative to fresh catalyst activity has been measured at various temperatures around the ABS dew point where the temperature has been either decreased or increased in steps of 5°C. The coal-fired case results are shown in *Figure 11*. The steady state activity relative to the uninhibited catalyst activities, k/k_0, is given as a function of temperature. When the temperature is lowered towards the bulk dew point, inhibition is observed from 320°C, 28°C above the bulk dew point. When the catalyst is heated, a hysteresis effect is seen since reactivation is slower than inhibition. It is actually necessary to bring the catalyst up above 350°C (60°C above the bulk dew point) to fully regenerate the catalyst. The Topsøe design model predicts an inhibition level that is an average between the observed levels at decreasing temperature and increasing temperature, respectively. Regeneration of a fully inhibited catalyst follows a curve (blue points in *Figure 11*) that is quite different from the regeneration of a catalyst partially inhibited at the design dew point temperature. However, in practical operation one should not operate the catalyst at temperatures close to the bulk dew point until 100% inhibition is reached.

The oil-fired experiment showed a tendency that inhibition levels also to some extent depended on the cooling rates. Inhibition was stronger when the catalyst was quench cooled, i.e. temperature was lowered to the design dew point from 360°C, compared to stepwise (5°C) cooling, cf. *Figure 12 on page 14*. During the cooling transient pore condensation develops in pores that are larger than the pores where ABS condenses at steady state conditions. Steady state is, however, never reached as a result of the hysteresis phenomenon, which means that once formed the condensate is more difficult to remove.

Before extracting the DNX-HD element from the test reactor the temperature was lowered to the design dew point (310°C) and given enough time to reach the steady state inhibition level. The elements were then characterized in order to describe the nature of the NH_4HSO_4 pore filling. The sample was analyzed for ammonium content and sulfur content. The pore-volume distribution and specific surface area were measured by multi-point (QBET) and single-point (HBET) nitrogen adsorption/desorption. Degassing temperature was set to 150°C for 48 hours in order to detain the ABS in the pore structure. The results are listed in *Figure 13* and *Figure 16* on pages 14-15. Up to 2.7 w% sulfur is accumulated in

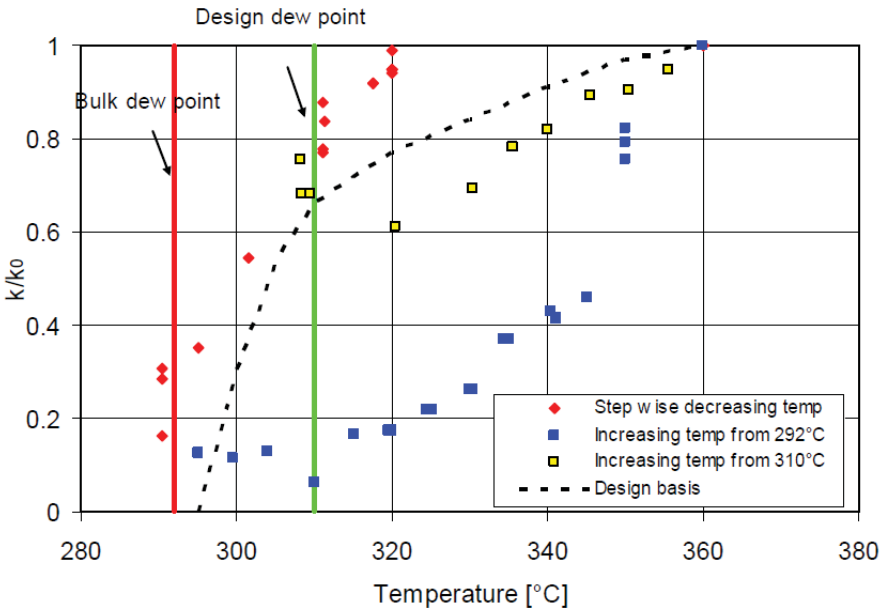

Figure 11: Steady state activity at operation close to the ABS bulk dew at typical coal fired conditions

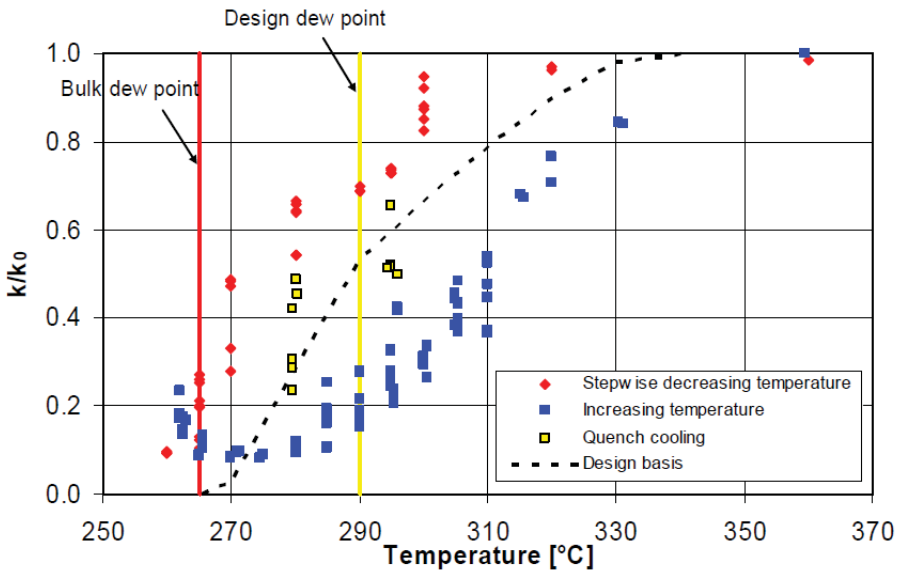

Figure 12: Steady state activity at operation close to the ABS bulk dew at typical HFO fired conditions

Position in catalyst [mm], from top	S [%w]	NH_4^+ [%w]	N/S molar ratio	Relative Specific surface QBET	Relative Nitrogen pore volume	Relative Specific surface HBET
0	2.70	0.48	0.32	-	-	-
100	1.37	0.34	0.46	0.49	0.73	0.50
250	0.82	0.12	0.28	0.69	0.93	0.42
350	0.67	0.07	0.22	-	-	-
500	0.62	0.06	0.19	0.78	1.00	0.71
ABS	23.1	9.92	0.77	-	-	-
Ref	0.01-0.05	-	N.A.	1.00	1.00	1.00

Figure 13: DNX-HD Experiment

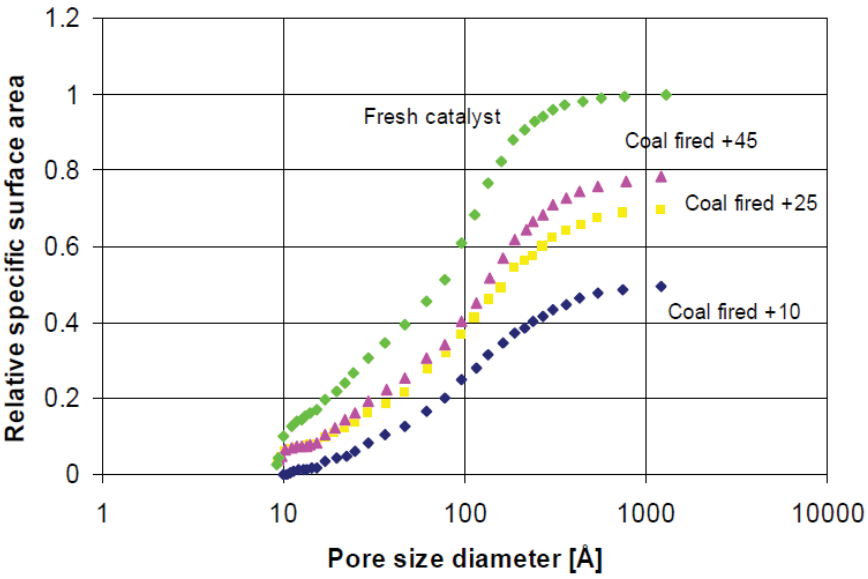

Figure 14: Cumulative specific surface area measured by nitrogen adsorption. The samples were taken at different distances, 10cm, 25cm and 45cm, respectively, from the leading edge of the catalyst.

the catalyst. The molar nitrogen-to-sulfur ratio, N/S ratio, is lower than the stoichiometry in NH_4HSO_4 (N/S = 1.0), which is explained by an absorption capacity of sulfuric acid in liquid ABS and sulphur adsorption in the catalyst. The background sulfur absorbed on the catalyst is 100-500 ppmw. In spent catalyst the background content is often higher due to the sulfatation of fly ash accumulated in the catalyst.

A piece of ABS taken from a cold surface in the reactor was analyzed and this sample had a N/S ratio of 0.77. The average ratio in the catalyst is 0.29.

The cumulative specific surface area shows how accessible surface area in the catalyst decreases as ABS condenses in the micropore structure. It is also seen that the surface area reduction is largest at the leading edge of the catalyst.

In the oil-fired boiler simulation the catalyst was extracted after operation at the design dew point temperature and a sample was taken from the leading edge for chemical analysis [1]. The catalyst was reinserted into the reactor. The catalyst was then regenerated and the temperature was subsequently decreased quickly to the bulk dew point. When complete inhibition had been obtained, the temperature was increased to the design dew point and the catalyst was then extracted and analyzed again [2].

The results show that the accumulated amounts of sulfur and ammonium at steady state to some extent depend on the temperature-time history of the catalyst. A quench cooling to the bulk dew point followed by an increase in temperature to the design dew point results in smaller amounts of accumulation compared to quench cooling directly to the design dew point. This indicates an effect of pore blocking in the outer pores of the pore structure as a part of the ABS inhibition mechanism. As in the DNX-HD experiment the nitrogen/sulfur ratio in the catalyst is around 0.30.

	Sample Position from leading edge	S [%w]	NH_4^+ [%w]	N/S molar ratio	Relative Specific surface area	Relative N_2 pore volume
Design Temp. Operation [1)]	+ 0	4.7	0.76	0.29	0.47	0.57
Bulk Dew point operation [2)]	+ 0	2.6	0.45	0.31	0.47	0.62

Figure 15: DNX-LD experiment

The decrease in vapor pressure of accumulated ABS could be explained by several mechanisms. One explanation could be that interactions between the condensed salt and the catalyst change the vapor pressure. Another explanation could be formation of $(NH_4)_2SO_4$ by reaction with gas phase ammonia. Ammonium sulfate has been shown to have a lower vapour pressure [2]. However, this explanation is not in line with the observed decrease in nitrogen/sulfur ratio in the catalyst. Finally, accumulation of sulfuric acid could play a role in the vapor pressure change.

ABS INHIBITION MODEL

A design model that predicts the effect of ABS inhibition including the dynamic behavior has been developed at Haldor Topsøe. The model consists of a number of differential equations describing the conversion of ammonia and NOx, coupled with the uptake and release of SO_3 from ABS which means that one molecule of NH_3 is released for every molecule SO_3 that is released. In the model SO_3 is calculated as sum of H_2SO_4 and SO_3, denoted SO_3. The catalyst has been sectionalized in the gas-flow direction and the pore condensation is assumed constant in these sections. The change in pore condensation is calculated in time steps based on the calculated gas phase outlet SO_3 concentration in each section. The model does not take SO_3 reactions with fly ash in the bulk or in the pores into account.

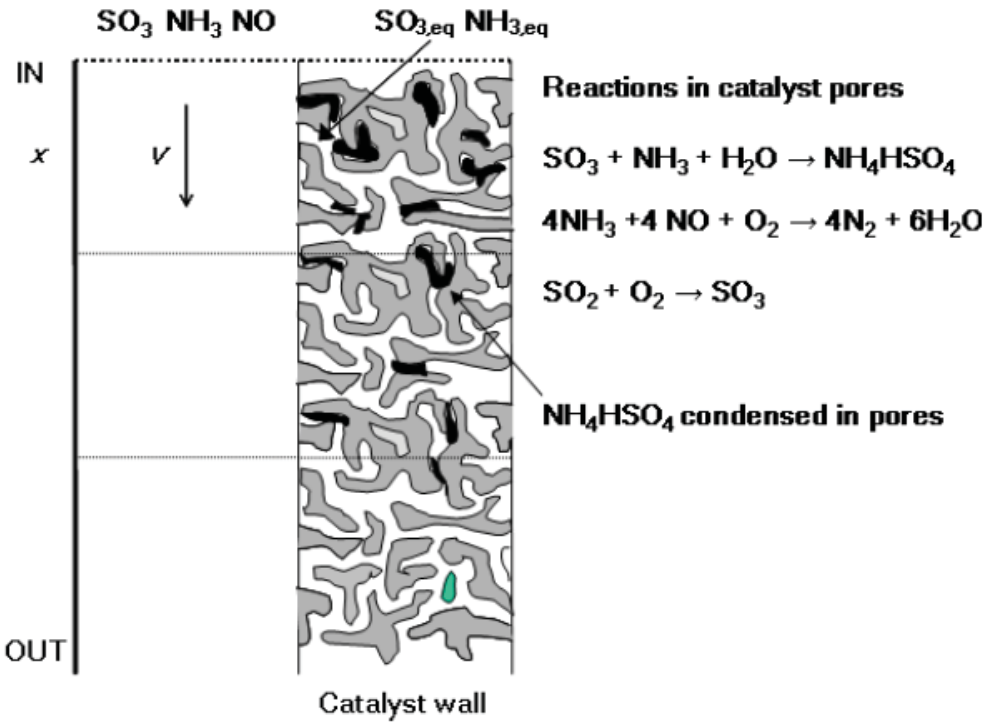

Figure 16: ABS deactivation mechanism. Bulk phase SO_3 and NH_3 condense in the catalyst pores where the SCR DeNOx reactions take place.

$$\frac{dP_{SO_3',cat}(x,t)}{dx} - \frac{k_g \cdot a}{v_0} \cdot \left(P_{SO_3',cat}(t) - P_{SO_3'}(x,t)\right) = 0 \quad , \quad 0 \le x \le l, \quad t \ge 0 \quad P_{SO_3'}(0,t) = P_{SO_3',0}(t)$$

$$\frac{dP_{NH3}(x,t)}{dx} + \frac{k_{NH_3} \cdot a}{v_0} \cdot P_{NH_3}(x,t) - \frac{dP_{SO_3'}(x,t)}{dx} = 0 \quad , \quad 0 \le x \le l, \quad t \ge 0, \quad P_{NH_3}(0,t) = P_{NH_3,0}(t)$$

$$\frac{dP_{NO}(x,t)}{dx} + \frac{dP_{SO_3'}(x,t)}{dx} - \frac{dP_{NH_3}(x,t)}{dx} = 0 \quad , \quad 0 \le x \le l, \quad t \ge 0, \quad P_{NO}(0,t) = P_{NO,0}$$

where the pore system partial pressure $P_{SO3,cat}$ is a function of the pore volume blocked by ABS, bulk species concentrations at the section inlet and the temperature:

$$P_{SO_3',cat}(t) = f(pv(t), P_{SO_3',0}, P_{NH_3,0}, P_{NO,0}, T) \quad , \quad t \ge 0$$

The change in blocked pore volume with time for each section is calculated as:

$$\left.\frac{d(pv)}{dt}\right|_t = \frac{\left(P_{SO_3'}(l,t) - P_{SO_3'}(0,t)\right) \cdot F \cdot M_{NH_4HSO_4}}{R \cdot T \cdot \rho_{NH_4HSO_4}} \cdot \frac{1}{m_{cat,section}} \quad , \quad pv(0) = pv_0 \quad , \quad t \ge 0$$

The intrinsic rate constant is assumed to be proportional to the fraction of accessible surface area:

$$k_i = \alpha \cdot k_{i,0}$$

The observed reaction rate constant kNH_3 is then calculated taking the relative influence of intrinsic chemical reaction and diffusion into account:

$$k_{NH_3} = \left(\frac{1}{k_g} + \frac{1}{k_i \cdot \eta_{cat}}\right)^{-1}$$

List of symbols:

a	: Specific geometric surface area [m^2/m^3]
F	: Volumetric flow rate in the monolith [Nm^3/h]
k_g	: External mass transfer coefficient [$Nm^3/(m^2 \cdot h)$]
k_i	: Intrinsic reaction rate coefficient [$Nm^3/(m^2 \cdot h)$]
k_{NH3}	: Observed reaction rate coefficient [$Nm^3/(m^2 \cdot h)$]
l	: Reactor bed length [m]
M	: Molar mass [kg/mole]
m	: Mass [kg]
v_0	: Empty reactor velocity [Nm/h]
P_i	: Partial pressure of component [N/m^2]
$P_{SO3,cat}$	: SO_3 partial pressure in pore system [N/m^2]
pv	: ABS filled pore volume [m^3/kg_{cat}]
R	: Gas constant [J/(mole·K)]
r_{pore}	: Pore radius [m]
T	: Temperature [K]
t	: Time [h]
x	: Axial position [m]
α	: Accessible surface area fraction
η_{cat}	: Catalyst effectiveness factor
$\rho_{NH4HSO4}$	: Density [kg/m^3]
σ	: Surface tension [N/m]

The effective diffusion coefficient for ammonia and NOx is assumed independent of the ABS condensation in the pore structure. The set of equations can be solved to provide the overall observed activity of the reactor bed length.

As shown earlier in *Figures 11 and 12* on pages 13 & 14 the prediction of the equilibrium ABS inhibition corresponds well to experimental observations. The observed dynamic behavior is also well described by the model which is shown by both laboratory experiments and in full scale as described in the next section. A model simulation of the inhibition in the DNX-HD coal-fired experiment shows that the model predicts a larger amount of ABS in the pore system compared to analysis of the extracted catalyst, cf. *Figure 17* on page 17. This indicates that the ABS does not solely affect the intrinsic activity but also the effective diffusion coefficient. Presumably the reason is that the activity is overestimated for a given amount of pore condensation. The agreement between pore-volume measurements and the ABS-filled pore volume estimated from chemical analysis is reasonable.

Position [mm] from top	From QBET analysis	S analysis	N analysis	Model prediction
100	53	54	17	74
250	14	17	4	64
500	~0	14	2	54

Figure 17: DNX-HD experiment, ABS pore volume (ul/g) in catalyst

HALDOR TOPSØE INDUSTRIAL EXPERIENCE

The possibility of operation near or below the ABS dew point has a number of advantages. In coal-fired boilers the SCR can be operated at reduced load at temperatures close to the bulk dew point for several days. Operation below the bulk dew point should never occur since the catalyst surface becomes sticky and initiates irreversible fly-ash deposition. In tail-end flue gases, i.e. after particulate removal, with very low concentrations of dust and SO_3, operation near or below the bulk ABS dew point is possible for an extended period (months). This is of relevance to e.g. SCR units on waste-incineration plants. An option for regeneration using a duct burner or steam has to be available.

In coal-fired boilers the SCR DeNOx activity can be maintained at a relatively high level during cyclic operation if the boiler is operated at reduced load for a limited time. The activity decreases around 15% during 72 hours at typical SCR conditions with 16 ppm SO_3, cf. *Figure 18*. As low-temperature operation typically occurs at reduced load, the reduced activity is sufficient to maintain the desired NOx removal efficiency.

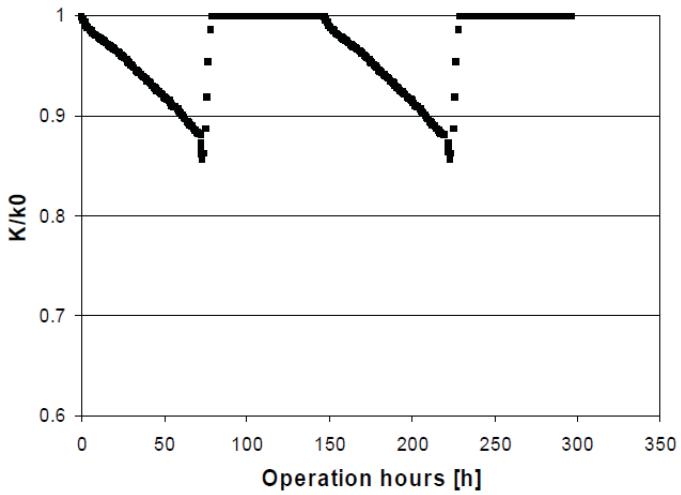

Figure 18: Predicted relative SCR DeNOx activity in 290° C /350° C cyclic operation of a coal fired boiler with 265 ppm NOx, 90% NOx removal, space velocity 1700 Nm³/m³/h and 16 ppm SO_3 at 290° C. The bulk dew point is 286° C. Regeneration takes place at 100% load conditions and 350° C.

The effect of operating close to the dew point can be minimized by increasing the amount of catalyst, e.g. by adding a catalyst layer. In *Figure 19* the effect of additional catalyst, corresponding to reducing the space velocity, on the overall steady state catalyst activity is shown. The relative activity loss close to the bulk dew point is lower the higher the design NOx conversion of the SCR unit since most of the ammonia is converted in the first layer. A catalyst with high porosity as the DNX® catalyst also reduces the effect of ABS close to the dew point because the catalyst can accommodate more ABS.

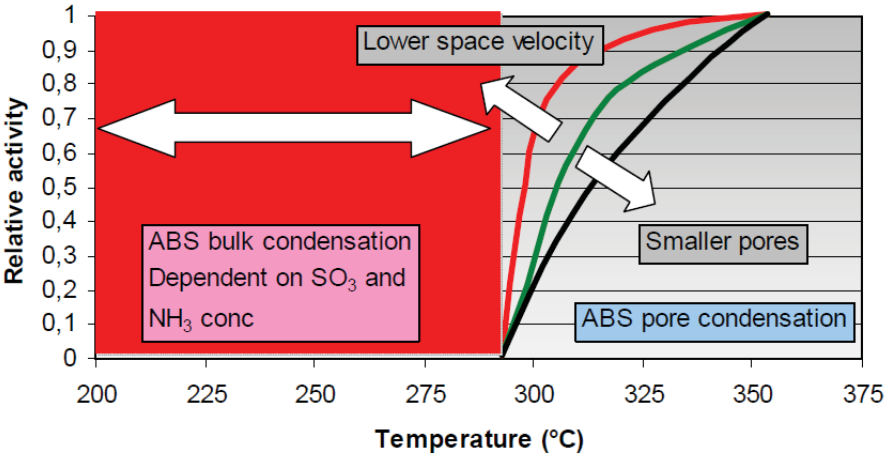

Figure 19: Effect of amount of catalyst, i.e. space velocity, on ABS inhibition on relative activity in the SCR close to the ABS dew point.

In tail-end SCR units with low SO_3 levels ABS may build up only slowly over time. In *Figure 20* on page 18 the DeNOx activity is given as a function of operating hours for a typical tail-end installation. With 0.5 ppm SO_3 70% of the DeNOx activity is retained after 2000 hrs.

One difficulty in designing SCR units for operation close to the dew point in real plants is the uncertainty in the estimation of the SO_3 concentration. When measured in high-dust SCRs the SO_3 concentration is often underestimated due to SO_3 capture in the sample-line fly-ash filter [4].

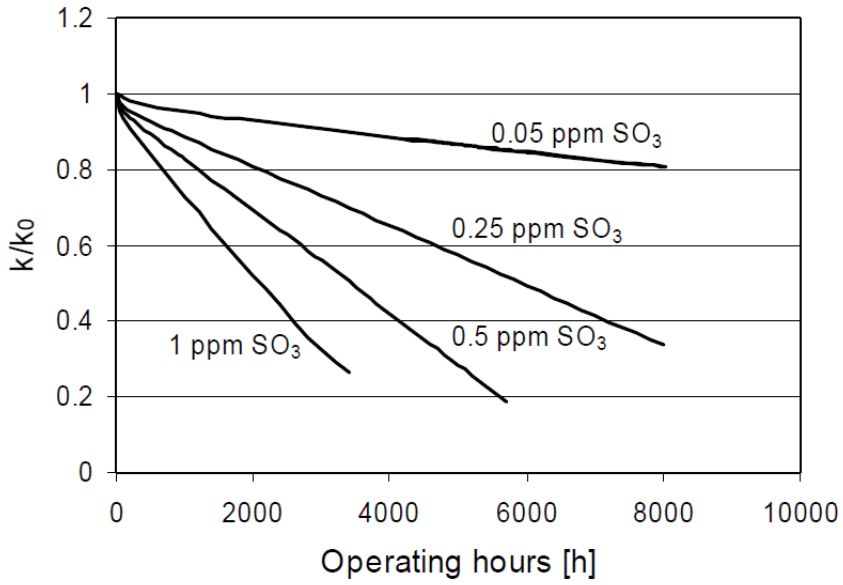

Figure 20: Predicted development in SCR activity as a function of SO_3 concentration in a tail-end unit. NHSV = 2800 h^{-1}, 250 ppm NOx, 80% DeNOx and 260° C.

At DONG Energy's Studstrup Power Plant in Denmark an ammonia injection strategy has been implemented at reduced load. 1% conversion of SO_2 in the boiler is assumed and the maximum allowable ammonia injection that gives a margin of 10°C to the Matsuda ABS dew point is calculated. As a result the minimum operating temperature can be reduced and the strategy takes the coal sulfur content into account. In order to monitor the operation more closely a continuous SO_3 monitoring system has been installed at the plant. The measuring principle is based on condensation/evaporation of condensables which is detected by electrical conductivity. The SO_3 level is then determined from the observed dew point. Breen Energy Solutions supplied the SO_3 probe. This technology is an alternative to the traditional method based on gas sampling and controlled condensation. To what extent the new method has been validated against the traditional method is unknown but the probe seems to provide reasonable but less accurate results.

A reduced-load and regeneration experiment was carried out at the plant. Initial baseline operation at 350°C ensures that the catalyst is completely emptied from ABS. This was followed by approximately 10 hours of operation below the catalyst dew point with a minimum temperature of 275°C. Finally the catalyst was regenerated at 350°C. The SO_2 level was approximately 500 ppm, giving an SO_3 level of 2-3 ppm if it is assumed that the observed SO_3 concentration corresponds to 0.5% oxidation of the SO_2. It is known that the actual observed SO_3 level corresponds to an apparently lower SO_2 conversion at low SO_2 levels (below around 1000 ppm SO_2) due to the sulfur oxide binding capacity of the fly ash. At higher sulfur levels approximately 1% SO_2 conversion is observed in the boiler. The 2-3 ppm level was also confirmed by the Breen probe. The SO_3 was monitored at the SCR outlet throughout the experiment and results are shown in *Figure 21*.

At temperatures below 325°C the SO_3 level drops to zero which indicates that all SO_3 is captured in the SCR as ABS. During regeneration SO_3 peaks of 25 to 33 ppm are observed.

Looking at the data a little more in detail reveals that the system behavior is captured by the HTAS dynamic ABS model. In *Figure 22* (on page 19) the data from *Figure 21* between 68 and 95 hours are shown. It is assumed that 3 ppm SO_3 is accumulated as ABS during the 10 hours of operation at reduced load which results in 0.007 ml ABS per gram catalyst in the reactor inlet. Using this pore-volume filling at the SCR inlet as an input to the simulation of the regeneration gives an estimated SO_3 peak that correlates quite well with the measured SO_3 peak. In the simulation shown in *Figure 22* it is assumed that the temperature is increased in steps first to 325°C and then to

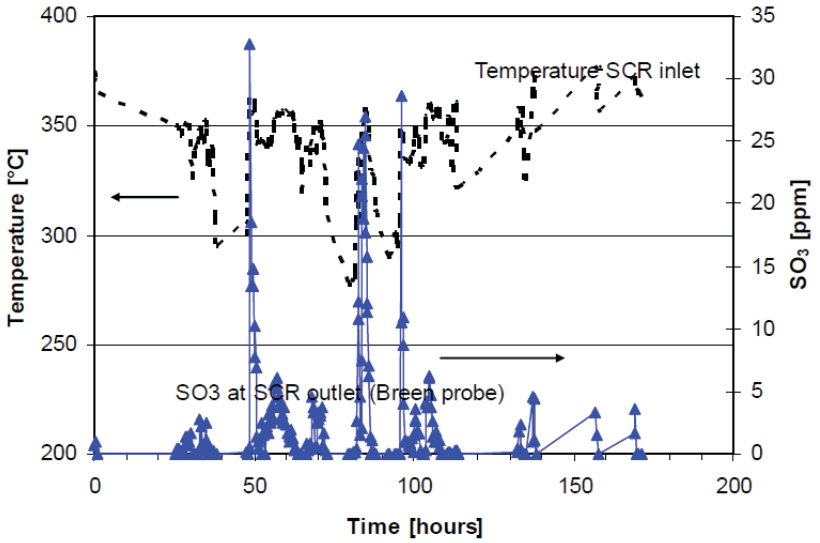

Figure 21: Temperature at SCR inlet and SO_3 level at SCR outlet during a reduced-load and regeneration experiment at Studstrup Power Plant 5

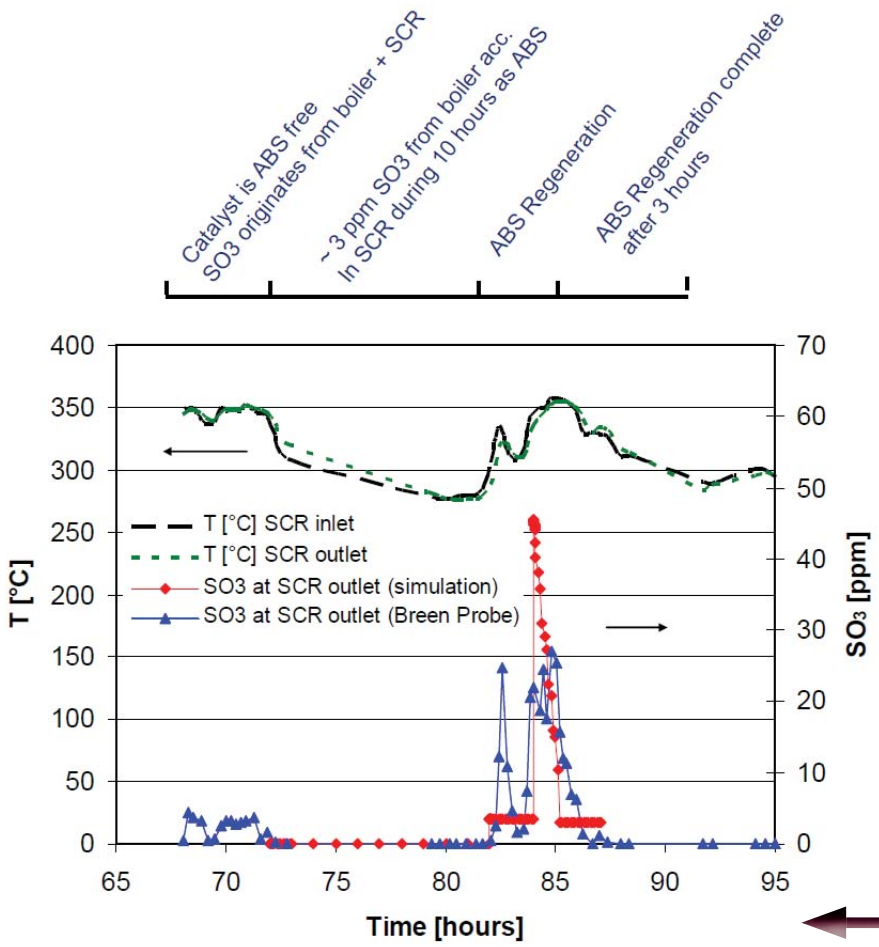

Figure 22: Measurements and simulation of SO_3 level at SCR outlet during a reduced load and regeneration experiment at Studstrup Power Plant 5.

350°C. This is the reason why the simulation does not follow the first peak. However, the peak size and duration predicted by the simulation is not very far from the measured dynamics. In *Figure 23* another example is shown. It is here clearly seen that complete regeneration is obtained after 4 hours at 350°C.

Actually ammonia injection has been carried out at temperatures down to 265°C at Studstrup Power Plant without any reported problems.

SUMMARY

The known dew point correlations for the formation of ammonium bisulphate have been confirmed by NOx conversion experiments that verified that steady-state catalyst activity approaches zero as the temperature approaches the predicted ABS bulk dew point. Due to capillary forces in the pore system an effect of ABS on the catalyst efficiency is observed from approximately 28°C above the bulk dew point. The steady-state and transient behavior of ABS inhibition is satisfactorily described by an inhibition model developed at Haldor Topsøe. A new finding is a hysteresis effect meaning that regeneration by heating of an ABS-inhibited catalyst to a certain activity level requires a higher temperature than the temperature at which this level is reached when the temperature is decreased from above the ABS dew point. Even when ammonia injection is stopped it is difficult to re-evaporate the last fraction of ABS in the catalyst pore structure at temperatures below 350°C.

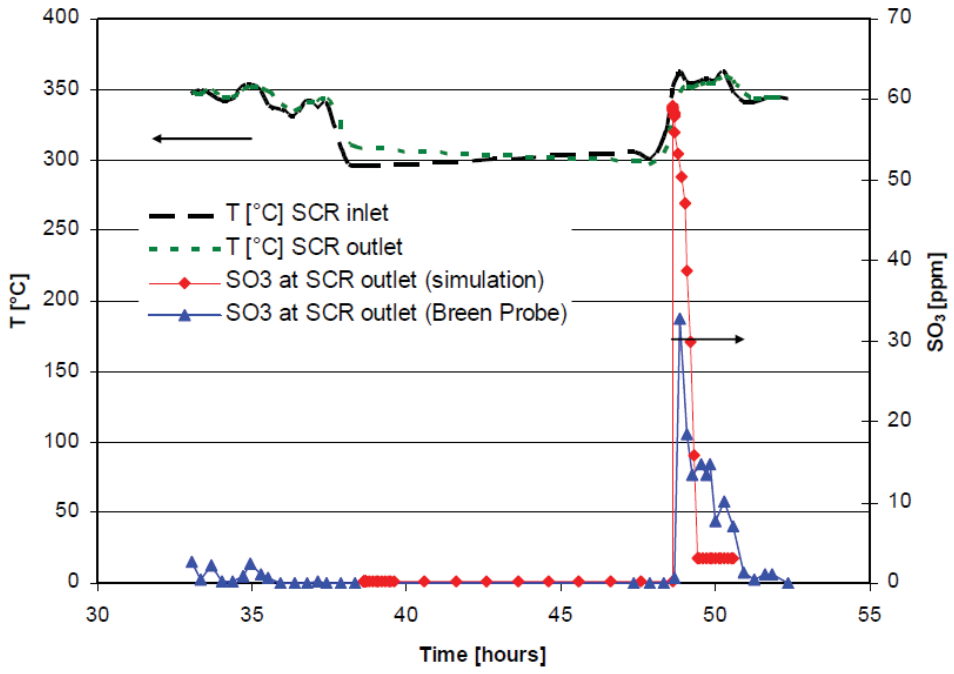

Figure 23: Measured and simulated SO_3 slip during reduced load operation at Studstrup Power Plant 5.

The DNX® catalyst, providing a high porosity, ensures optimal resistance to ABS inhibition and by applying Haldor Topsøe's design tools, SCR DeNOx operation close to the ABS dew point can be safely utilized to the maximum possible extent. At DONG Energy's Studstrup Power Plant in Denmark an ammonia-injection strategy based on the design tools described in this paper has been implemented with success. The dynamic behavior has been monitored using a probe for SO_3 measurements and corresponds well with the behavior predicted by the ABS-inhibition model.

REFERENCES

1. Matsuda, S., Kamo, T., Kato, A. and Nakajima, F., Ind. Eng. Chem. Prod. Res. Dev., 1982, 21, 48-52.
2. Burke, J.M. et al., Ammonium Sulfate and Bisulfate Formation in Air Preheaters, 1982.
3. Ando, Jumpei. NOx Abetement for Stationary Sources in Japan. EPA-600/7-79-205 EPA Contract No. 68-02-2161, 1979.
4. Nielsen, M.T., Importance of SO_2 Oxidation to High Dust SCR DeNOX Units, NETL Conference on NOx Control Technologies 2003.
5. Data received from Dong Energy, 2009.

For further information
contact Nate White at
Nathan.White@am.umicore.com

Umicore acquires Haldor Topsoe's Stationary Catalyst Businesses

Umicore has acquired the heavy duty diesel and stationary catalyst businesses of Haldor Topsoe. Haldor Topsoe is a producer of high performance catalysts for a wide range of industries. Its automotive catalysts are used in emission systems for on-road and non-road heavy-duty diesel applications. Its stationary business offers catalytic solutions to treat NOx emissions from industrial sources such as gas-fired power plants as well as marine applications.

Pascal Reymondet, Executive Vice-President Catalysis, said: "The business is highly complementary with Umicore, particularly through its focus on cutting edge technology, operational excellence and sustainability." The agreement included all employees and all technologies, intellectual property rights, and production and R&D facilities belonging to the two business areas in Denmark, USA, China and Brazil.

High Reactivity Hydrated Lime for Heat Rate Improvement

Written by Charles A. Lockert, Mississippi Lime Company

ABSTRACT

With the implementation of MATS, depressed natural gas prices and an increasing emphasis on renewables, traditional coal-fired generating assets are looking for flexible solutions to improve operating efficiency. One avenue for efficiency gains could come from a hydrated lime dry sorbent injection system -- shifting the focus of the DSI system from a regulatory need to a source of operational and overall cost benefit to the user.

As with many plants in the Eastern U.S., the subject plant has moved to higher sulfur, lower cost fuel. To mitigate the negative effect of high SO_3 levels that come from combustion and subsequent flue gas SCR oxidation, the plant chose to inject hydrated lime ahead of the air heater. Prior to this study, plant operating practices were designed to minimize the amount and cost of hydrated lime usage. This article outlines the benefits and cost implications of increasing, rather than minimizing, hydrated lime usage for overall commercial improvement.

INTRODUCTION & INITIAL OBJECTIVE

The Utility identified for this study is located in the Midwestern U.S. near large deposits of Illinois Basin Coal. The fuel currently burned averages 3% sulfur, 13% ash and has a HHV between 10,500 and 10,750 BTU/Lb. Additionally, plant operating history shows that the air heater has a higher propensity for fouling than most plants.

To combat the negative effects of sulfuric acid and ammonia salt deposits in the air heater, the plant chose to place its hydrated lime injection location at the SCR Outlet and placed a Breen AbSensor probe at the air heater inlet for feedback and control. In addition, the plant chose to use High Reactivity Hydrated Lime (HRH), an enhanced hydrate that is designed for fast and efficient in-flight capture of acidic pollutants such as SO_3. A targeted, continuous, hydrate feed rate of 500 Lb/Hr. was implemented. Combining the positive effects of pre-AH hydrate injection with traditional usage of steam coil air preheaters, the plant was able to avoid any forced outage time due to air heater fouling or pluggage. To further improve operating profits, the plant looked to optimize/reduce total hydrated lime usage through feedback from the Breen probe.

BASELINE CONDITIONS

The Figure below shows feedback from the Breen probe on the state of the condensable material in the flue gas during

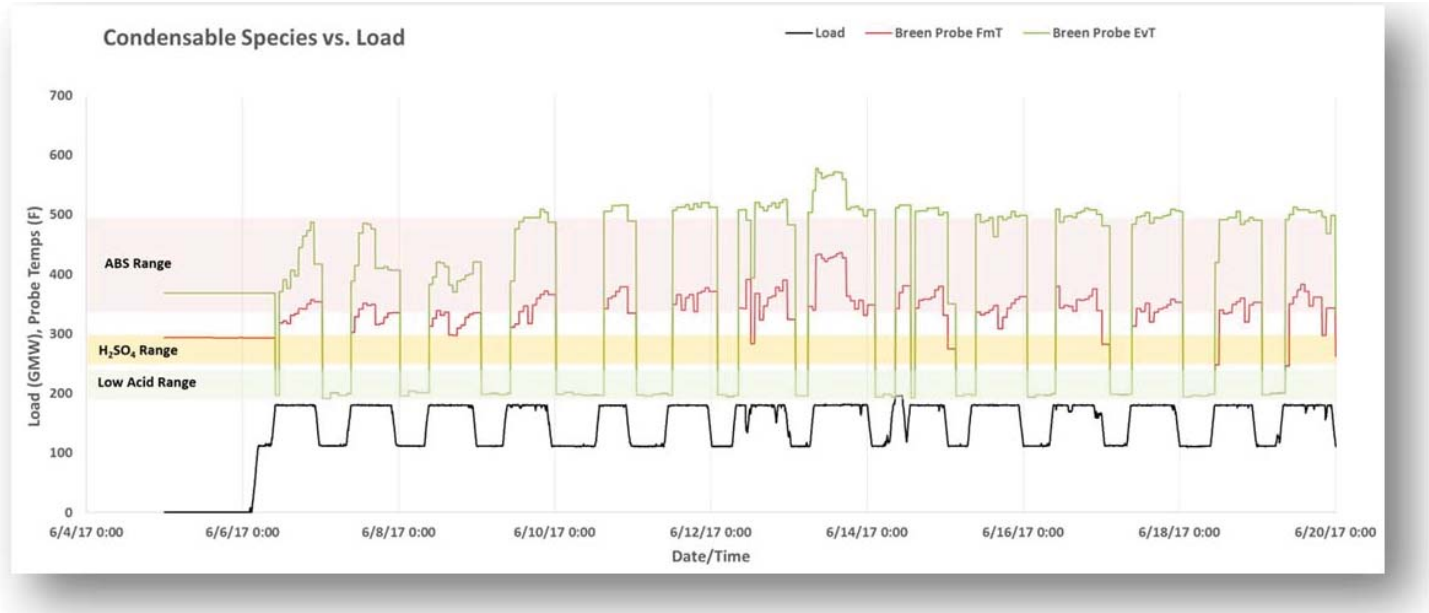

Figure 24: Flue Gas Evaporation and Formation Temperature vs. Unit Load

baseline plant operating conditions. The red and green lines are the formation and evaporation temperature of the detected condensable species and the black line is the associated load. To keep deposits in the portion of the air heater that is reliably cleaned through normal sootblowing practices, both the red and green lines should reside in the orange band associated with sulfuric acid.

As can be seen, at low load the flue gas exhibits no detectable condensable material and at high loads the material is firmly in the Ammonium Bisulfate range (nominally 330°F to approximately 500°F). The plant's hydrated lime process, targeted at 500 Lb/Hr., seems to have been over-treating at low loads and undertreating at high loads. In an effort to minimize sorbent usage at low loads and to reduce the severity of deposits at high loads, the plant moved to a practice of 750 Lb/Hr. at high load and 300 Lb/Hr. at low load.

LOOKING AT THE LARGER PICTURE

Presented in *Figure 25* is a theoretical plot of the SO_3 concentration at the AH Inlet as a function of increasing load. The calculations assume that the SCR ammonia injection is

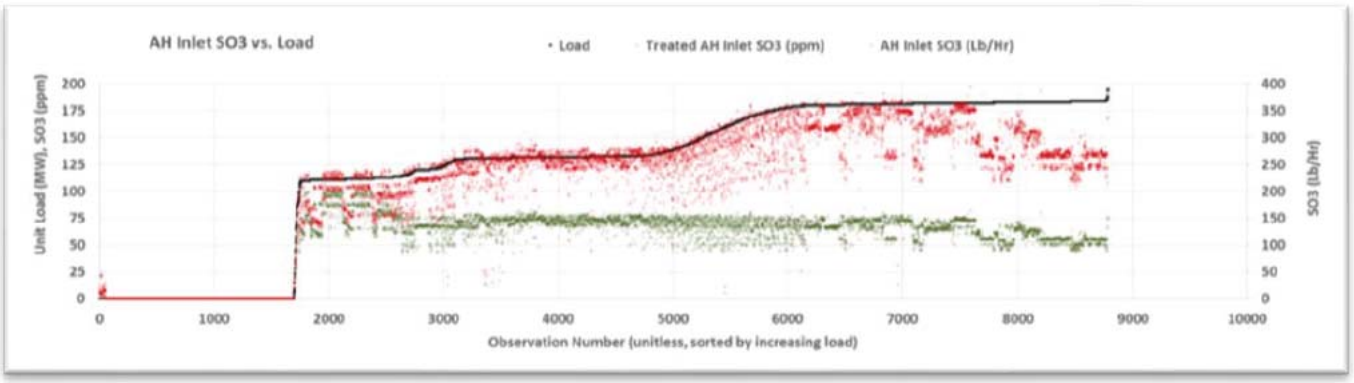

Figure 25 - Projected SO_3 vs. Load

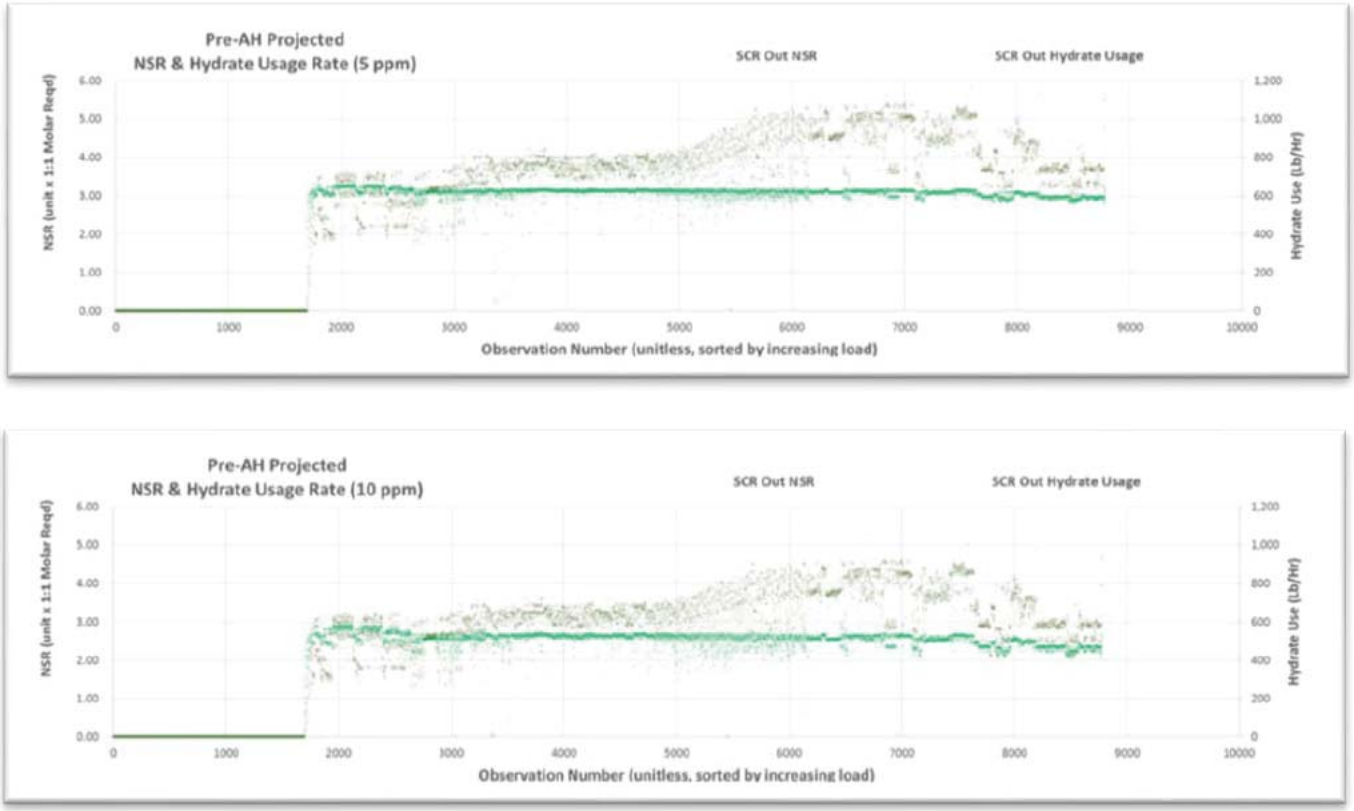

Figure 26 - Projected Hydrate Metrics for Target

OFF. As can be seen in the plot, the projected values move between 50 and 75 ppm (250 – 350 Lb/Hr.) of SO_3. Plotted on the previous page are two graphs (*Figure 26*) showing the theoretical hydrated lime usage to reduce SO_3 concentration to levels of 10 ppm and 5 ppm respectively. In summary, the calculations predict a nominal level of 1,100 Lb/Hr. to achieve 5 ppm and 900 Lb/Hr. to achieve 10 ppm.

This data tells us that mitigation of the SO_3, in the absence of ammonia at full load, will require between 900 Lb/Hr. and 1100/Lb/Hr. The current plant operating practice is insufficient to treat the acid present at full load and, without supplemental heat from the steam coils, air heater deposition and fouling could occur.

In fact, the plant's air heater runs relatively free from differential pressure buildup so the steam coils are doing most of the work.

STEAM COIL USAGE

Figure 27 shows the total power (green trace) supplied to the plant's steam coil air heater system to raise the air heater outlet gas temperature to a base level of 310°F at low load and roughly 340°F at full load. Extrapolation of this data over the entire operating year and valuing it based on the cost of the fuel to generate this power shows that the plant historically pays over $180,000 to mitigate air heater fouling due to ammonia salt formation in the baskets.

WHEN MORE IS LESS

The original objective of the project was to determine how to optimize the use of hydrated lime to reduce total sorbent usage. Close study of the data revealed that reducing the hydrated lime feed rate would only result in increased steam coil power consumption to mitigate air heater fouling. In fact, the optimum solution was to increase hydrated lime usage to the point that supplemental heat input from the steam coils was not required.

Figure 28 (on the next page) is a non-temporal observation plot of the condensable formation/evaporation conditions at full load compared to variable hydrate lime feed rates. Inspection shows that there are three distinct condensable regimes corresponding to varying feed rates.

- High Level ABS corresponding to feed rates below 300 Lb/Hr.
- Mixed Acid and ABS corresponding to feed rates between 300 Lb/Hr. and 900 Lb/Hr.
- Low Level Acid corresponding to feed rates above 1,100 Lb/Hr.

CONCLUSIONS

The initial project objective was to determine a real-time method to minimize hydrated lime feed rates using the Breen probes for feedback. As the project unfolded it became obvious that a more profitable objective would be:

- Use the Breen probes for feedback, AND
- Use increased hydrated lime to reduce the AH Inlet SO_3 to a point where the steam coils were unnecessary

Figure 27 – Power for AH Steam Coil Operation

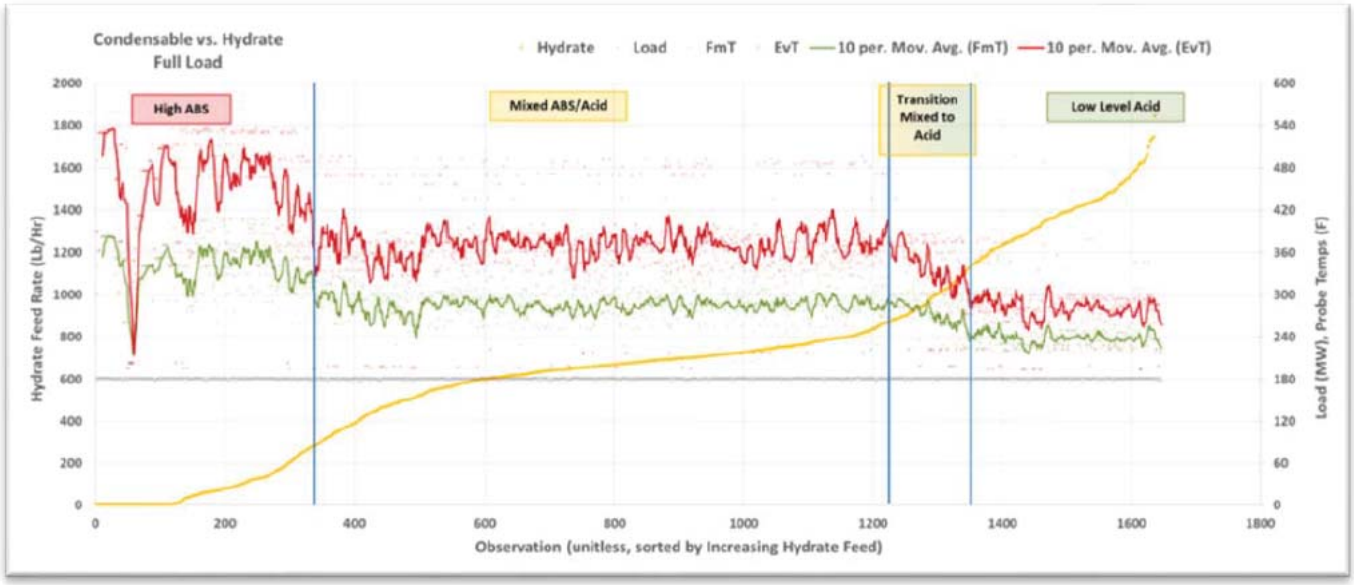

Figure 28: Hydrate Required for Condensable Species Change

That objective is met by:

- Increasing the full load hydrate injection rate by 350 Lb/Hr. to a level of 1,100 Lb/Hr., and
- Reducing the low load hydrate injection rate by 200 Lb/Hr. to a level of 100 Lb/Hr.

The result of increasing the total hydrated lime feed rate at full load, reducing the feed rate at low load and eliminating steam coil usage results in an immediate cash flow improvement 2-3 times the cost of the increased sorbent usage.

Co-benefits of reduced steam coil maintenance, reduced AH Outlet gas temperature and reduced back end corrosion are significant and only serve to increase the value of the plant's choice to change condensable control practices.

Following conclusion of the winter generating season the plant is exploring a move of the injection location from pre-AH to pre-SCR to capture improved unit turndown possibilities using the same levels of hydrate lime usage.

For further information
contact Cal Lockert at CALockert@MLC.com

BIOGRAPHY

Charles (Cal) Lockert currently heads the Integrated Performance & Optimization team at Mississippi Lime Company following the acquisition of Breen Energy by Mississippi Lime in 2015. Prior to that, Cal was the President of Breen, a supplier of technology and process knowledge for measurement and control of sulfate based condensables in utility flue gas. Prior to joining Breen he has over 25 years experience in developing and commercializing new technologies for environmental and efficiency improvement in coal fired generating stations. Cal has a degree in Electrical Engineering and currently resides in Cleveland, Ohio.

Optimizing the Glenarm Station Gas Turbine OTSG Through Flow Modeling and Testing

Written by Kevin W. Linfield, Ph.D., P.E., Matthew R. Gentry, and Kanthan Rajendran, P.E. of Airflow Sciences Corporation

INTRODUCTION

In order to work towards energy independence and produce efficient, reliable, environmentally responsible electricity, the City of Pasadena California embarked on the $137 million "Glenarm Repowering Project". As part of this project, the 50-year old steam generating unit was to be replaced with a new combined-cycle 71 MW power generating unit featuring a new gas turbine, steam turbine, once-through steam generator (OTSG), cooling tower, and 125-foot tall stack (Figure 29).

Figure 29: Glenarm Power Station

In 2014, Innovative Steam Technologies (IST) of Cambridge, Ontario was awarded the contract to provide the once-through steam generator. IST hired Airflow Sciences Corporation of Livonia, Michigan to perform Computational Fluid Dynamic (CFD) flow modeling and flow testing to aid in the design of the OTSG.

Due to California's stringent emissions standards, IST had Airflow Sciences perform a detailed CFD model that included all aspects of the OTSG performance. The model thus simulated all flow characteristics including the turbine exhaust gas velocity patterns, pressure losses through the ducting, thermal mixing of the tempering air system, as well as the ammonia injection system. Additionally, to ensure the most accurate results and to help validate the CFD model, Airflow Sciences conducted field testing to measure flow properties at the turbine outlet, CO catalyst inlet, Ammonia Injection Grid (AIG) inlet, SCR catalyst inlet, and stack.

GLENARM FACILITY

The new Glenarm unit is an OTSG capable of running in combined cycle and simple cycle operation. It features a GE LM6000 PG gas turbine and the OTSG is equipped with both a CO and an SCR catalyst for emissions control. There is tempering air injection upstream of the OTSG plenum for flue gas temperature control during simple cycle operation. The AIG injects vaporized ammonia that reacts in the SCR catalyst to remove NOx.

CFD FLOW MODELING

The modeling was performed with Airflow Sciences Azore® CFD software, a 3-D finite volume polyhedral flow solver (www.AzoreCFD.com). The model domain extended from the gas turbine outlet through to the stack exit (*Figure 30*). The flow inlet condition was based on both turbine-supplier data and Airflow Sciences field test data. The model included the internal geometry features that affect the flow such as the tempering air lances, structural supports, CO and SCR catalyst, OTSG steam tube banks, and silencer.

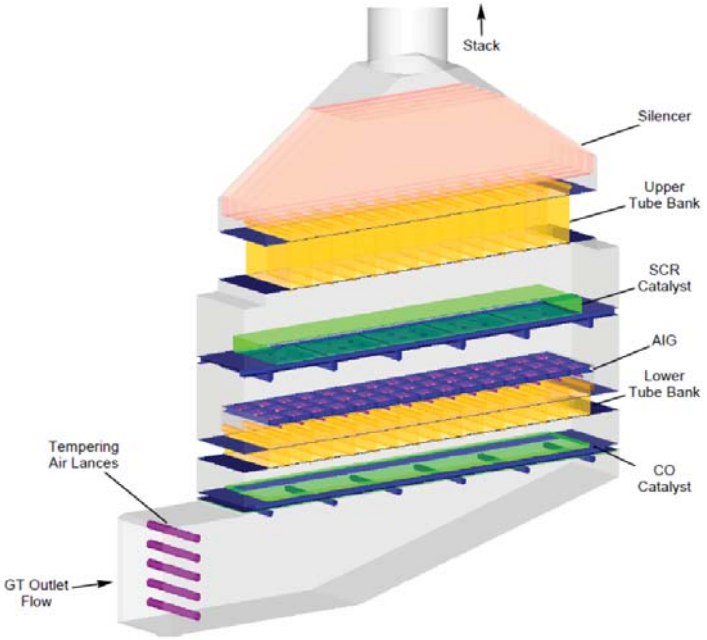

Figure 30: OTSG CFD Model Geometry

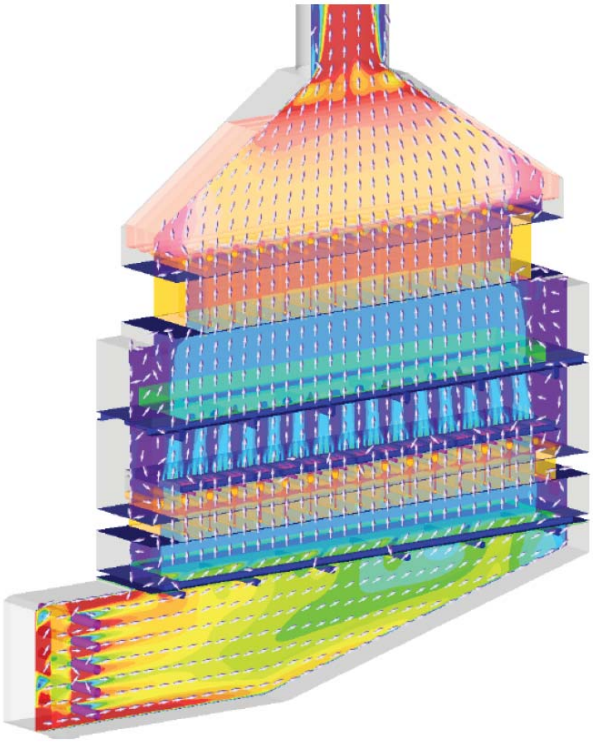

Figure 31: CFD Model Velocity Patterns

The CFD simulations with the Azore software provide a wealth of flow-related data to quantify system performance. This includes velocity patterns, pressures, temperature distribution, mixing of the tempering air with the hot exhaust gases, and tracking of the injected ammonia. Typical CFD results showing the velocity patterns are provided in *Figure 31*.

Due to the relatively short mixing time between the AIG and the SCR catalyst, estimated to only be about 0.3 s, the original design had a relatively poor ammonia distribution, with a uniformity of about 27%RMS (*Figure 32*). A typical performance goal is to have ammonia uniform at less than 10%RMS.

In order to maximize ammonia mixing in the short distance available, Airflow Sciences used the CFD model to design flow control devices to direct the exhaust flow optimally over the AIG nozzles, and static mixers to increase ammonia dispersion. Working with IST, the AIG nozzle pattern was also modified to take advantage of the static mixers. The resulting modifications resulted in a much improved ammonia distribution at the SCR catalyst, with a predicted RMS of about 6% (*Figure 33*).

The CFD modeling effort also included design modifications to reduce temperature stratification going through the unit, which can result in uneven catalyst performance. For operating conditions that required the use of the tempering air system, areas with high and low temperatures were observed in field test data and in the CFD modeling of the initial configuration, with a variation of over +/- 50ºF at the CO catalyst test ports (*Figure 34* on page 27). The flow devices and static mixers designed by Airflow Sciences, as well as modifications to the tempering air injection lances, resulted in a more uniform temperature distribution entering the CO and SCR catalysts. The temperature variation at the CO catalyst in the final design configuration was predicted to be within +/-20ºF (*Figure 35* on page 27).

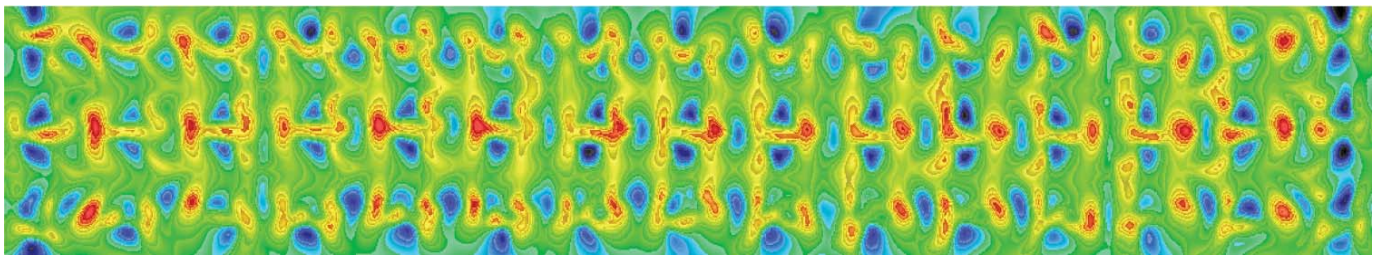

Figure 32: Original Design Ammonia Distribution at SCR Cata;yst Inlet - 27.1%RMS

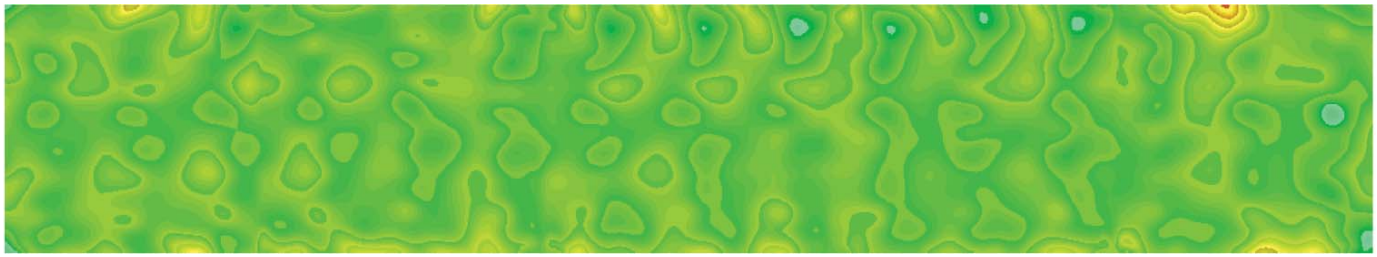

Figure 33: Final Design Ammonia Distribution at SCR Catalyst Inlet - 6.2%RMS

Figure 34: Original Design temperature Distribution at the CO Catalyst Inlet

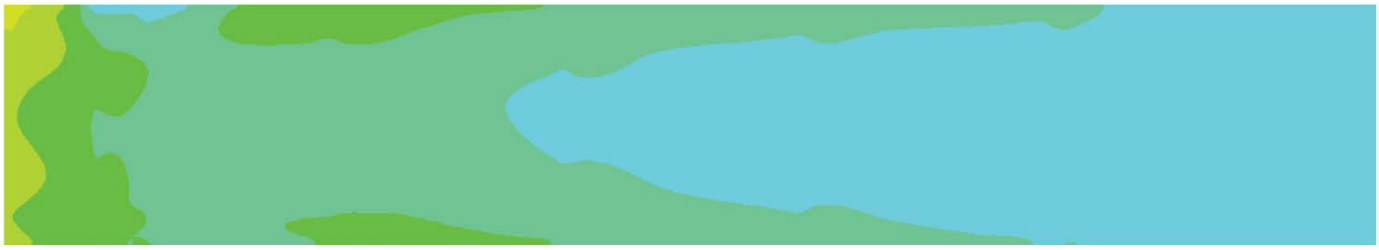

Figure 35: Final Design temperature Distribution at the CO Catalyst Inlet

FIELD TESTING

During start-up testing but prior to performance testing, the unit was experiencing some NOx emission issues. As a follow up to the CFD flow modeling, Airflow Sciences performed field testing to determine the as-constructed flow distributions. The data from the tests were then used to help validate the CFD model and to enhance the design to optimize the ammonia distribution and unit performance.

Testing was conducted in the ductwork downstream of the LM6000 turbine, upstream of the CO catalyst, upstream of the AIG, upstream of the SCR catalyst, and in the stack. Velocity and temperature measurements were conducted at each test plane. Testing was completed at Full Load, in both Simple Cycle and Combined Cycle operation, as well as at Minimum Load, Simple Cycle operation.

At all locations, the velocity and temperature profiles were measured using a 3D type pitot probe. The 3D probe test procedure (40 CFR Part 60 Appendix A, Method 2F) allows both the angle of the flow as well as the magnitude of the velocity to be determined. The 3DDAS™ data acquisition system was used to log the data and ensure accurate results.

Due to the high temperatures and velocities at the gas turbine outlet, a custom-built water-cooled 3D probe was used at this location. Airflow Sciences designed and fabricated the probe. With the liquid cooling system, the probe is able to

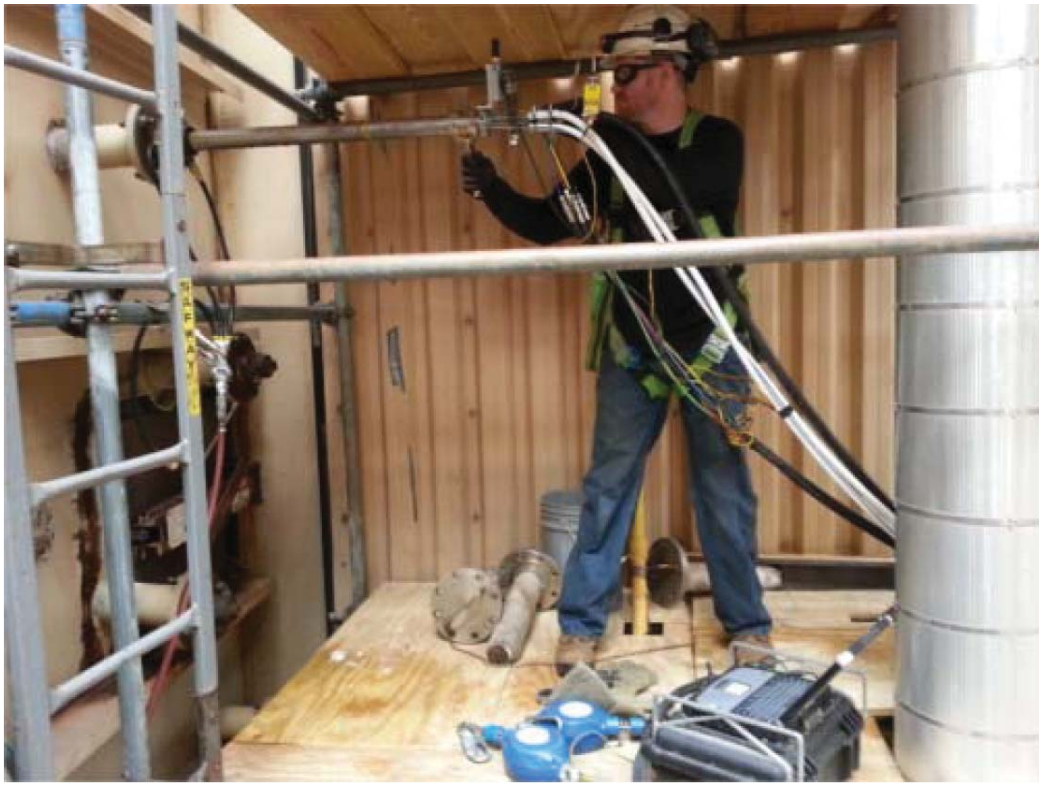

Figure 36: Water-cooled 3D Velocity Probe and 3DDAS Data System

withstand the very high flue gas temperatures downstream of the turbine without being compromised. The probe has a larger outer diameter as well, leading to improved stiffness and reducing the chances of probe deflection and vibration. Figure 36 on page 27 shows the probe in use.

The test data gathered at the turbine outlet were incorporated into the CFD model as an inlet boundary condition. The downstream test data were used to validate the CFD model, as CFD model predictions could be compared to the field test data at the CO catalyst inlet and AIG planes.

Testing confirmed a temperature imbalance issue that was seen in the CFD model results, and it was eventually determined that the tempering air system was not operating optimally. Temperatures near the SCR catalyst limit were recorded. Improving the temperature uniformity would prolong catalyst life and improve catalyst performance in general (this was addressed via the CFD modeling).

DESIGN MODIFICATIONS

Based on results of the CFD flow modeling and the field testing, the final recommended design featured modifications to the tempering air system, a variable porosity perforated plate, a flow straightener, flow control baffles, and a custom-designed static mixer. IST installed these modifications during 2016.

Figure 37: OTSG at Glenarm Station

PLANT OPERATIONS

In Q4 2016, the Glenarm unit underwent the official performance test. The boiler passed all the contractual requirements, such as steam production, pressure drop and noise. Emissions on CO, NOx and ammonia slip were within the stringent limits under simple and combined cycle operation over the operating range of the unit. Both CO and NOx were within the 2 ppm limit while ammonia slip was under 5 ppm.

Mr. David Lai, P.Eng., Project Manager for IST, commented "The CFD, flow testing and flow optimization have helped IST enhance the performance of the tempering air system and improve tremendously the ammonia distribution and mixing needed for the unit to meet such tight emission limits specified in the Glenarm Repowering project."

For further information
contact Kevin Linfield at klinfield@airflowsciences.com

BIOGRAPHY

Dr. Kevin W Linfield, P.E., P.Eng., is the Engineering Director at Airflow Sciences. He received his B.A.Sc., M.A.Sc., and Ph.D. degrees in aerospace engineering at the University of Toronto. With over 25 years of engineering experience, Dr. Linfield enthusiastically tackles flow-related problems and offers practical, cost-sensitive solutions. An avid outdoorsman, when not in the office, Dr. Linfield can be found on the water or in the field.

Mr. Matthew R Gentry, received his M.S.E. in Aerospace Engineering from the University of Michigan in 2004, with a specialization in structural mechanics. He has worked for Airflow Sciences for over 13 years, performing flow modeling as well as both laboratory and field testing. He has served as project manager for HRSG, SCR, and sorbent injection projects, helping to optimize pollution control performance in industrial applications. mgentry@airflowsciences.com

Mr. Kanthan Rajendran, P.E., is a Project Engineer and has been with Airflow Sciences for 9 years. He conducts field testing and flow modeling of various industrial and power generation equipment, including gas turbines, baghouses, SCRs, and ESPs. He has a M.S.E. in Aerospace Engineering from the University of Michigan. srajendran@airflowsciences.com

Airflow Sciences Corporation

WELCOME

New WPCA Corporate Sponsors

United Conveyor Corp

Kevin McDonough

UNITED CONVEYOR CORPORATION

KraftPowercon

Paul Leanza

KRAFT POWERCON

WesTech

Jake Blattman

WESTECH

Evoqua

Max Swoboda

EVOQUA WATER TECHNOLOGIES

WPCA

High Frequency TR Set (HFTR) Performance Comparison with Mid Frequency TR in Cement Plant Application

Written by Elavarasu Jayakumar , Stock Equipment

Figure 38: Side view of the three-field ESP

Schenck Process Solutions India Pvt Ltd (SPG) received an order to replace conventional TR set with high frequency TR set (HFTR) on Unit-8 of Shree Cements Limited (SCL) in RAS, Rajasthan. Prior, this facility installed (1) mid-frequency controller (MFTR) on Unit-3 with mixed results. This article will show the differences in operation and collection efficiencies between the MFTR and the HFTR.

This facility has a capacity of 3000 TPD and utilizes three-field Electrostatic Precipitators on each of their clinker coolers to control emissions. The clinker coolers were originally equipped with Him-Enviro Electrostatic Precipitator (ESP) powered by conventional TR sets operating at 50 Hz.

The ESP was originally designed for a gas flow rate of 126.94 m^3/s, with a maximum inlet dust concentration of 40 g/Nm^3 and outlet emission of <50 mg/Nm^3 when all fields are in operation. However, prior to the modifications, the plant could only reach an outlet emission of 87mg/Nm^3.

Shree Cements Limited previously installed one mid-frequency controller on Unit-3, operating at 200Hz, onto the

Before MFTR

Location	Date	Sampling Time	Value Observed (mg/Nm3)	Kill feed (TPH)	AQC Status	Recirculation Damper	Stack Damper	TR1		TR2		TR3		Remarks
								kV	mA	kV	mA	kV	mA	
Unit-III Cooler ESP	05.09.2017	12:20PM-01:00PM	55	239	In-Circuit	0%	100%	37	168	41	912	43	685	With Old System (Single Phase Conventional TRSET)
	05.09.2017	01:15PM-01:55PM	62	239	In-Circuit	0%	100%	36	157	41	950	42	650	
	14.09.2017	03:40PM-04:15PM	72	238	In-Circuit	0%	100%	39	283	41	1098	46	938	
	14.09.2017	04:25PM-04:55PM	61	238	In-Circuit	0%	100%	38	270	40	870	45	912	
Average Sampling(mg/Nm3)			63											

After MFTR

Location	Date	Sampling Time	Value Observed (mg/Nm3)	Kill feed (TPH)	AQC Status	Recirculation Damper	Stack Damper	MFTR-1		TR2		TR3		Remarks
								kV	mA	kV	mA	kV	mA	
Unit-III Cooler ESP	19.09.2017	03:35PM-04:11PM	52	224	In-Circuit	0%	100%	43	146	33	544	41	744	With New System (MFTR in (1st) first field only)
	19.09.2017	04:10PM-04:47PM	47	224	In-Circuit	0%	100%	42	120	28	217	36	464	
	20.09.2017	03:40PM-04:10PM	47	230	In-Circuit	0%	100%	46	128	38	834	39	970	
	20.09.2017	04:20PM-04:50PM	49	230	In-Circuit	0%	100%	45	142	37	801	43	921	
Average Sampling(mg/Nm3)			48.75											
Percentage of Reduction in dust emission (%)			22	Reduction by Installation of Mid frequency TRSET in 1st field only										

Figure 39: Emission Measurements & Operating Parameters before and after MFTR installation.

existing inlet TR set to increase the average operating voltage of the ESP. *Figure 39* on page 30 shows the emission measurements and operating parameters of the Unit-3 Cooler ESP before and after the MFTR installation.

Figures 40 and 41 graph the kV & mA before and after the MFTR was installed. There is only a minor change in both secondary voltage (kV) and current (mA) compared to when only conventional TR sets were in operation. There is slight improvement in the secondary voltage on the 1st field, but the 2nd and 3rd fields don't have any improvement. *Figure 39* shows the change in the ESP performance. Overall, there is a 22% PM reduction, but the emissions are still over the required maximum limit.

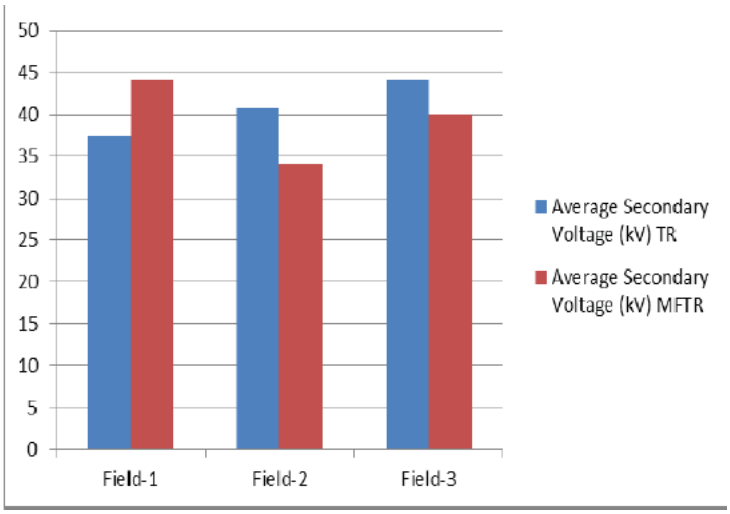

Figure 40: Secondary kV before and after MFTR

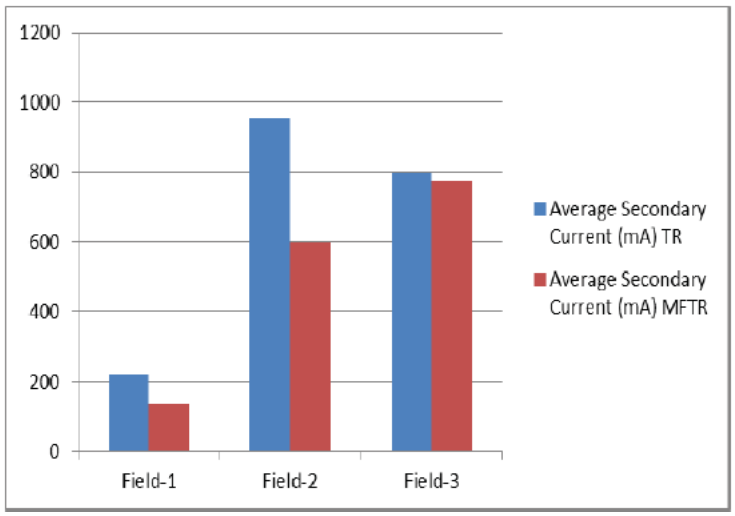

Figure 41: Secondary mA before and after MFTR

Shree Cement Limited contacted SPG to discuss potential solutions to meet the government emission regulations. SPG was able to utilize their process expertise to provide the customer with performance estimates for a variety of scenarios. The confidence generated by this analysis prompted the customer to quickly exercise the proposed solution.

Schenck Process provided a complete solution which included an ESP inspection and rectification services bundled with (1) 60kw/67kV/900mA HFTR. In March 2017 the new power supply was commissioned at Shree Cement's Unit-8 clinker cooler ESP.

After the HFTR installation, the outlet PM emission achieved 42mg/Nm^3, well below the original 80mg/Nm^3 and within the government limits The ESP performance improvement was 47.2% with (1) HFTR installed. (See *Figure 43* on page 32)

The HFTR is able to achieve these results by supplying a constant voltage to the ESP versus the original conventional TR sets or MFTR. This eliminated unwanted peaks in the output voltage waveform that caused excess sparking and poor performance. With this more constant output voltage, the HFTR was able to introduce more current into the ESP for better charging which led to better collection efficiency and lower PM emission.

Figure 42: HFTR (ModuPower™ MPX) installed on the roof of ESP

Before HFTR

Location	Date	Sampling Time	Value Observed (mg/Nm3)	Kill feed (TPH)	AQC Status	Recirculation Damper	Stack Damper	TR1		TR2		TR3		Remarks
								kV	mA	kV	mA	kV	mA	
Unit VIII Cooler ESP	02.04.2017	11.52AM-12:28AM	82	241	In-Circuit	0%	100%	29	137	30	237	28	300	With Old System (Single Phase Conventional TRSET)
	02.04.2017	12:43PM-01.21PM	77	241	In-Circuit	0%	100%	41	136	40	236	36	300	
Average Sampling(mg/Nm3)			80											

After HFTR

Location	Date	Sampling Time	Value Observed (mg/Nm3)	Kill feed (TPH)	AQC Status	Recirculation Damper	Stack Damper	HFTR-1		TR2		TR3		Remarks
								kV	mA	kV	mA	kV	mA	
Unit VIII Cooler ESP	25.05.2017	01:26PM-01:59PM	47	230	In-Circuit	0%	100%	51	518	46	458	41	464	With New System HFTR in (1st) first field only
	19.07.2017	04:34PM-05:09PM	49	239	In-Circuit	0%	100%	51	571	46	528	42	537	
	24.07.2017	12:45PM-01:18PM	35	239	In-Circuit	0%	100%	51	542	47	528	44	539	
	28.07.2017	11:42PM-12:15PM	37	252	In-Circuit	0%	100%	52	571	48	529	44	537	
Average Sampling(mg/Nm3)			42											
Percentage of Reduction in dust emission (%)			47.2	Reduction by Installation of High Frequency TRSET in 1st field only										

Figure 43: Emission Measurements & Operating Parameters before and after HFTR installation.

Figures 44 and 45 graph the secondary kV & mA before and after the HFTR was installed. The HFTR increased the secondary voltage (kV) and secondary current (mA) drastically in the 1st field. The HFTR performance impacts the 2nd and 3rd fields as well, as there is improvement in the kV & mA of the existing single phase 50Hz conventional TR sets. Per the data in *Figure 43*, this leads to overall higher collection efficiency to reduce the emissions. The emission has been reduced from an average of 80mg/Nm^3 to 42 mg/Nm^3 with only one HFTR installed on the Unit-8 cooler ESP. Overall, there is a 47.2% PM reduction.

Summary:

The mid-frequency controller designed for 400Hz operates at 200Hz and requires a 50% de-rate of the existing conventional TR set. There are higher losses when operating the existing 50 Hz TR set at mid-frequency, therefore higher power consumption when compared to the HFTR, which is designed to operate at high frequency. The mid-frequency TR uses series resonance which requires a new CLR so the mid-frequency inverter can vary output voltage through modulation. The causes higher stress on the inverter. The mid-frequency TR operates using soft switching, which waits for a zero-crossing condition to operate the IGBT.

Following the above performance tests, the high frequency TR set shows a greater improvement in the performance of the ESP when compared to the mid-frequency TR set. As shown in *Figure 46*, there is a 47% improvement for the HFTR vs. a 22% improvement for the MFTR. These results can be attributed to an increase in secondary voltage and current into the ESP due to a more constant secondary voltage.

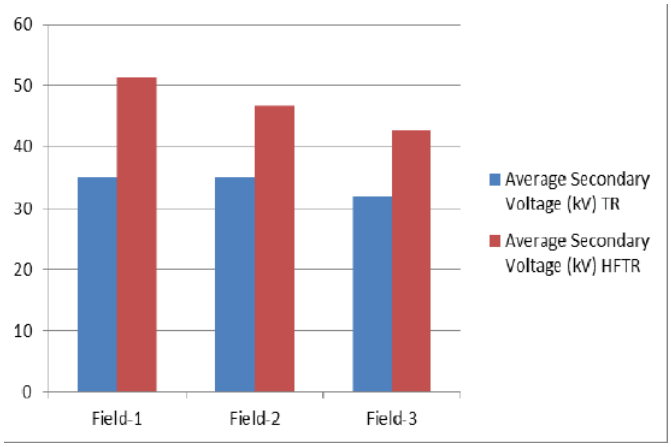

Figure 44: Secondary kV before and after HFTR

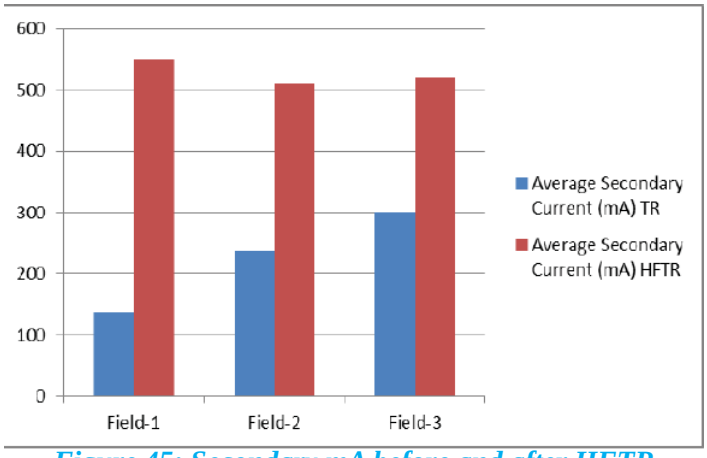

Figure 45: Secondary mA before and after HFTR

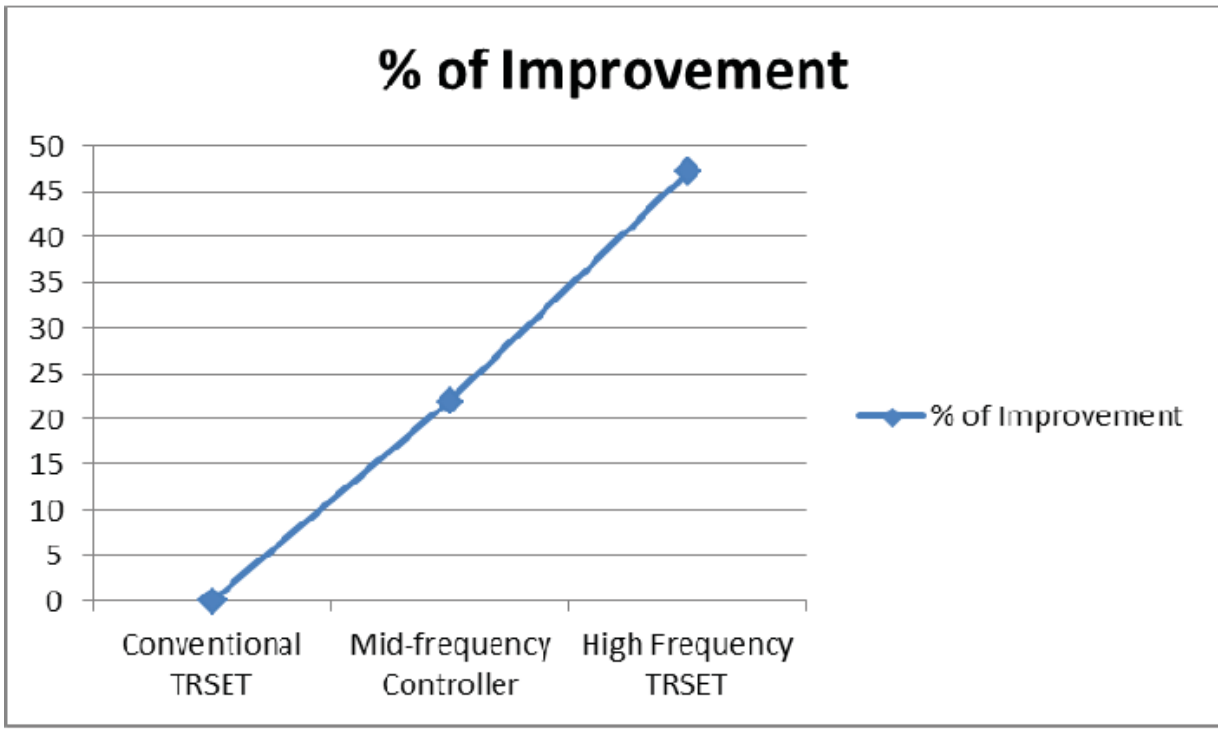

Figure 46: Comparison of % of improvement in Emissions

For further information
contact Elavarasu Jayakumar at
j.elavarasu@schenckprocess.com

BIOGRAPHY

Elavarasu Jayakumar is the Asst.Manager for the Environmental Controls product line at Schenck Process Solutions India Private Limited. Stock Equipment Company and Schenck Process India are part of the Schenck Process Group. With over 9 years of experience, Elavarasu is responsible for end to end process of Environmental Control Products for various industrial segments such as power, cement and sugar industries in India and South East Asia. Mr. Elavarasu holds a Bachelor of Engineering degree in Electronics and Communication from Anna University, India. He can be reached for questions or comments via email (j.elavarasu@schenckprocess.com) or phone at +91-8971666623.

Development of SCR Catalyst Regeneration Process for Enhanced Mercury Oxidation

Written by Thies Hoffmann, Xin Liu, Nick Pollack, Mike Mattes Cormetech Inc, Tobias Schwämmle and Thorsten Dux, STEAG Energy Services GmbH.

ABSTRACT

The removal of mercury from flue gas in wet scrubbers is greatly increased if the flue gas mercury (Hg) is present as a water-soluble oxidized species (e.g. Hg^{2+}). Increased mercury oxidation upstream of wet scrubbers improve the overall mercury removal with minimum additional costs. The selective catalytic reduction (SCR) catalyst in a fossil fuel power plant plays a key role as a co-benefit for oxidizing elemental mercury. However, there are influencing factors like the ammonia/ NOx ratio, which reduces the performance of regular SCR catalysts related to mercury oxidation.

Currently the SCR catalyst Original Equipment Manufacturers (OEMs) have provided enhanced mercury oxidation catalysts to the coal-fired power plants for reducing stack Hg emission[1]. To the SCR catalyst regeneration industry, developing enhanced Hg oxidation regenerated catalyst is important to help power plants further cost savings on NOx and Hg removal. Cormetech has developed proprietary regeneration methods to optimize regenerated SCR catalysts Hg oxidation. A systematic study in a laboratory micro reactor has been performed to evaluate regenerated SCR catalysts mercury oxidation. The test results demonstrated that SST's regenerated SCR catalysts performed well when compared to the OEM enhanced Hg oxidation catalyst. Furthermore, regular deactivated SCR catalyst was converted to enhanced Hg oxidation catalyst by means of the SCR catalyst regeneration process.

INTRODUCTION

Mercury emissions are of global concern due to their persistence, long-range mobility in the atmosphere, bio-accumulation in aquatic ecosystems and their neurotoxic impact on human health.[2,3,4] In January 2013, an intergovernmental negotiation committee convened by the United Nations Environment Programme (UNEP) agreed on the "Minamata" Convention, a global treaty to reduce global mercury emissions.[5] The same year, the U.S. Environmental Protection Agency updated the emission limits of Mercury and Air Toxics Standards (MATS), where total emission of mercury from new coal-fired units burning low rank virgin coal must be controlled below the level of 0.003 lb./GWh.[6]

Mercury exists in three forms in the flue gas of coal-fired power plants namely particulate bound mercury (Hg^P), oxidized mercury (Hg^{2+}) (mostly mercury chloride ($HgCl_2$)) and elemental mercury (Hg^0).[7] *Figure 47* [8] shows a typical boiler configuration consisting of SCR-DeNOx-catalyst, electrostatic precipitator (ESP) and a wet flue gas desulfurization system (FGD) with the corresponding mercury behavior flow balance. Mercury is released from coal combustion in its elemental form (Hg^0). As flue gas cools, oxidized mer-

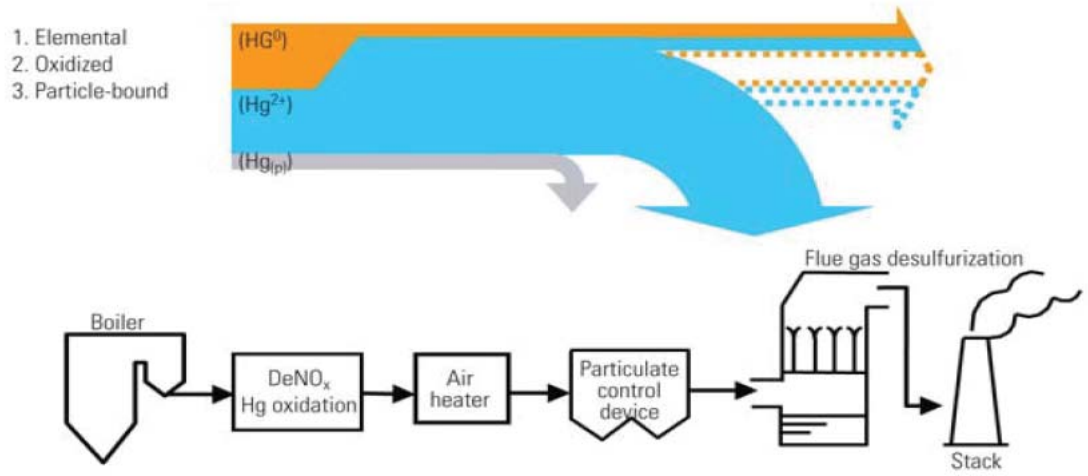

Figure 47: The behavior of mercury HG in a typical coal fired power plant

cury (Hg2+) forms due to the lower flue gas temperatures.[9] When the oxidized or elemental mercury contact with fly ash, some adsorbs on the fly ash depending on its composition. Fly ash and thus Hg^P are removed in the electrostatic precipitator. After the precipitator, the wet flue gas desulfurization is the major sink for oxidized mercury, due to the high-water solubility of $HgCl_2$.[10] However, Hg^0 is difficult to remove because of its high volatility and water-insolubility. Therefore, methods for mercury removal from the flue gas focuses on manipulating Hg^0.

There are two methods for elemental mercury control: adsorption and oxidation. Powder activated carbon (PAC) injection has proven to be an effective adsorption method for mercury removal in waste incinerators.[11] In coal-fired power plant Hg control, PAC is injected into the flue gas upstream of the ESP or baghouse. The Hg in flue gas is adsorbed by PAC and collected in the ESP or baghouse. But this method is expensive[12], and moreover the fly ash which contains a large amount of carbon is generally not available for beneficial reuse.[13] Therefore, significant attention has been placed on Hg^0 oxidation. The main idea behind mercury oxidation is to oxidize elemental mercury by either catalysts or oxidants in the flue gas. Subsequently, the oxidized mercury could be easily captured by wet flue gas desulfurization device (WFGD). [14,15,16]

In recent years, SCR DeNOx reactors have been extensively used in coal-fired plant to control NOx emissions.[17] Typical commercial SCR catalyst for coal-fired power plants is a vanadium oxide supported on titanium-based ceramic material.[18] Vanadium is the main active component in the SCR catalyst for NOx reduction. The SCR plays a key role as a co-benefit for oxidizing elemental mercury into its oxidized form. However, there are influencing factors such as the ammonia ratio applied for NOx-removal, which reduces the performance of catalysts related to mercury oxidation. In the presence of NOx and ammonia, the following three net reactions have been identified as relevant for the mercury chemistry over the SCR:

- R1: $2\ NO + 2\ NH_3 + ½\ O_2 \leftrightarrow 2\ N_2 + 3\ H_2O$
- R2: $2\ HCl + Hg^0 + ½\ O_2 \leftrightarrow HgCl_2 + H_2O$
- R3: $2\ NH_3 + 3\ HgCl_2 \leftrightarrow N_2 + 3\ Hg^0 + 6\ HCl$

Reaction R1 is the DeNOx reaction, R2 is the overall reaction of the oxidation of Hg^0 by O_2 and HCl and reaction R3 is the reduction of $HgCl_2$ with NH_3. [19]

To reduce NH_3 negative effect on Hg oxidation in SCR reactor, SCR catalyst OEMs are developing and promoting enhanced mercury oxidation catalysts to the coal-fired power plants to enhance SCR co-benefit for Hg control.

Regeneration processes removes catalyst deactivation compounds and can restore catalyst activity back to the original OEM level. As one of the first companies to develop catalyst regeneration, Cormetech has refined the process with our patented regeneration methods. Our selective impregnation process minimizes SO_2 to SO_3 conversion while achieving high catalyst activity levels to match original catalyst performance in demanding applications.

Finally, our testing for mechanical strength has become the EPRI standard. The modules go through a multi-stage process after arriving at the facility:

- Cleaning to remove fly ash and other particles which cause pluggage
- Immersion in a series of chemical baths to remove deposits that reduce performance
- Undergoes Selective Impregnation®, restoring full catalyst activity by infusing the module surfaces with oxides of base metals (V_2O_5 and either MoO_3 or WO_3)
- A heated drying process that re-establishes mechanical strength and fixation of the active metal oxides

Currently, different proprietary methods for improving Hg oxidation have been applied into the catalyst regeneration process. A systematic study in a laboratory micro reactor has been performed to evaluate SCR catalyst mercury oxidation. Various chemical compounds have been studied and applied into our catalyst regenerated process for improving Hg oxidation.

Figure 48: Bench scale reactor

LAB TEST FACILITIES

Bench test facilities can provide critical performance metrics that the SCR reactor owner/operator requires to make informed decisions.

Testing services can include:

- Bench scale reactor testing of full-size samples for activity (initial activity Ko, actual activity Kact), SO_2 / SO_3 conversion rate, pressure drop (*Fig 48 on page 35*)
- Micro scale reactor testing for small size catalyst coupons
- XRF analysis for surface and bulk composition of catalyst's substrate
- SEM analysis - catalyst surface scan
- BET / Pore Volume Analysis
- Hg Oxidation Testing

Figure 49: Hg oxidation testing lab in Herne, Germany

Hg OXIDATION TESTING SYSTEM

An Hg oxidation micro reactor system is used for measuring the Hg oxidation performance of catalyst samples. It is a fully automated and continuous system capable of injecting a wide variety of gaseous and aqueous species and measuring DeNOx, SO_2 oxidation and Hg^0 oxidation. A picture of the STEAG reactor system is shown above in Figure 49. The catalyst sample of up to 3 x 3 channels and 300mm in length is placed in a reactor made of borosilicate glass, which is installed in a heated oven. N_2, O_2, NO, NO_2, SO_2, NH_3, and Hg^0 are injected as gases, and H_2O, HCl, are injected as vaporized liquids. Hg^0 and Hg^{2+} concentrations are measured by a continuous Hg analyzer. A schematic of the system is shown in Figure 50 on page 37. [20]

Hg^0 and total mercury (Hg^T) were measured separately. To measure the elemental Hg, a Dowex® resin adsorbs Hg^{2+} before the flue gas sample is analyzed. Since Hg continuous emission monitoring systems (CEMS) only detect elemental Hg, for the Hg^T measurements, a tin(II) chloride ($SnCl_2$) solution is used to convert all Hg^{2+} to Hg^0 before sample gas gets into Hg CEM detector. The oxidized Hg is calculated by the difference between Hg^T and Hg^0. A schematic of Hg^T and Hg^0 measurement are shown in *Figure 50* on page 37.

TEST PLAN

According to the EPRI guidelines and in conjunction with the STEAG micro reactor and measurement system, Hg oxidation test conditions were developed to simulate the range of conditions that enhanced Hg oxidation catalyst might be utilized. The test matrix described below was then used to evaluate the performance of OEM enhanced oxidation catalyst and regenerated catalyst samples. The following flue gas characteristics were established and fixed throughout the test program:

- 50 µg/m^3 (STP, dry) elemental Hg
- 0.75 m/s flue gas linear velocity (LV)
- 3% O_2
- 8% moisture
- 1000 ppm SO_2
- 300 ppm NO

The following parameters were varied in the test program to simulate the range of conditions the catalyst would be expected to perform under

- Temperatures (350 °C and 380 °C)
- HCl concentrations (10ppm, 50ppm)
- NH_3 concentrations (0ppm, 120ppm)

Higher temperature low HCl conditions were intended to simulate Powder River Basin (PRB) coal applications while lower temperature high HCl conditions were intended to simulate high sulfur bituminous coal applications. The high ammonia condition of 120 ppm was intended to simulate the "average" or midpoint ammonia concentration across the top layer of catalyst in the reactor. The standard approach used on full length/full bench tests was considered but oxidation rates were too low at low HCL levels to provide meaningful data to evaluate differences in catalyst performance. The zero-ppm ammonia value was intended to simulate the bottom layer in the reactor.

The complete test matrix is summarized in *Figure 51* on page 37.

TEST RESULTS and DISCUSSION

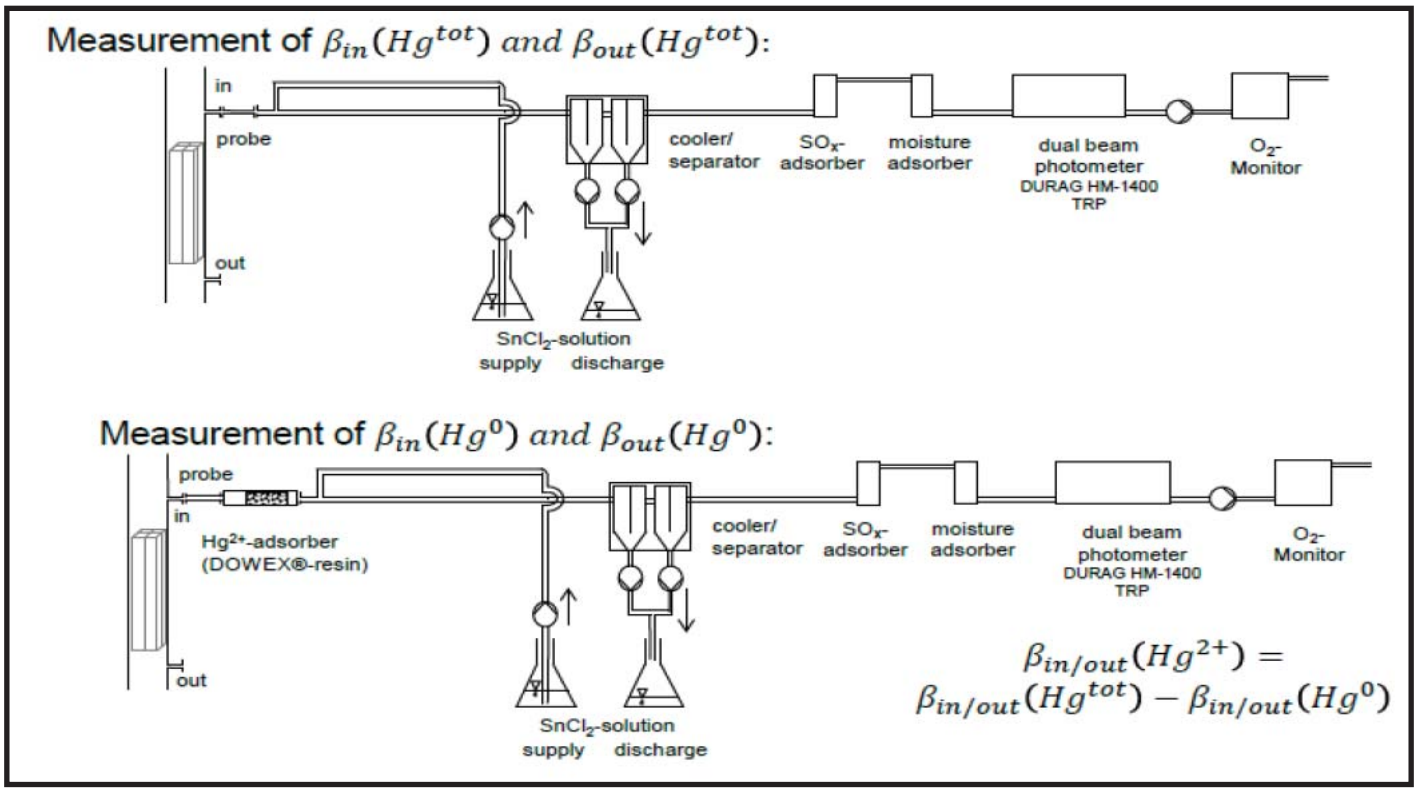

Figure 50: A schematic of Hg^T and Hg^0 measurement

First phase testing was conducted to compare Hg oxidation differences between a new commercial enhanced Hg oxidation OEM new catalyst (Reference Catalyst) and a new regular OEM catalyst (Catalyst 0) under the designed test conditions. Both were honeycomb catalyst. The two catalyst samples were prepared to 2x2 channels with 200mm length. Eight condition tests were conducted, and the results presented in *Figure 52* on page 38. Some of the key finding were:

- The Reference Catalyst shows better Hg oxidation than the Catalyst 0
- Both Reference Catalyst and Catalyst 0 show significantly reduced Hg oxidation under 120ppm NH_3 testing condition compared to 0ppm NH_3 present in the flue gas sample. Reference catalyst shows significant improved Hg oxidation than Catalyst 0 with 120ppm NH_3 present.
- 10ppm HCl test condition Hg oxidation result shows

Test-#	T	LV	AV	O_2	H_2O	NO	NH_3	SO_2	SO_3	HCl	HBr	CO	Hg^0	Hg^{2+}
[-]	[°C]	[m/s]	[m/hr]	[vol.-%]	[vol.-%]	[ppm]	[ppm]	[ppm]	[ppm]	[ppm]	[ppm]	[ppm]	[µg/m³]	[µg/m³]
0	con-ditioning													
1	380	0,75	21,1	3	8	60	0	1000	0	50	0	0	50	0
2	350	0,75	21,1	3	8	60	0	1000	0	50	0	0	50	0
3	380	0,75	21,1	3	8	60	0	1000	0	10	0	0	50	0
4	350	0,75	21,1	3	8	60	0	1000	0	10	0	0	50	0
5	380	0,75	21,1	3	8	300	120	1000	0	50	0	0	50	0
6	350	0,75	21,1	3	8	300	120	1000	0	50	0	0	50	0
7	380	0,75	21,1	3	8	300	120	1000	0	10	0	0	50	0
8	350	0,75	21,1	3	8	300	120	1000	0	10	0	0	50	0

Figure 51: Hg oxidation test matrix

less than 50ppm HCl condition.

- Under 10ppm HCl conditions, 380°C reactor temperature show less Hg oxidation than 350 °C reactor temperature.
- Under 0ppm NH_3, 50ppm HCl test conditions, temperature effect on Hg oxidation was minimized. Here 50ppm HCl plays the key role than higher temperature.

The first phase test tells us how NH_3, temperature and HCl influence Hg oxidation on the two catalyst samples. The Reference Catalyst is capable of improving Hg oxidation under both with and without ammonia. Furthermore, Reference Catalyst demonstrates significant Hg oxidation improvement compared to Catalyst 0 when ammonia was present. The questions were:

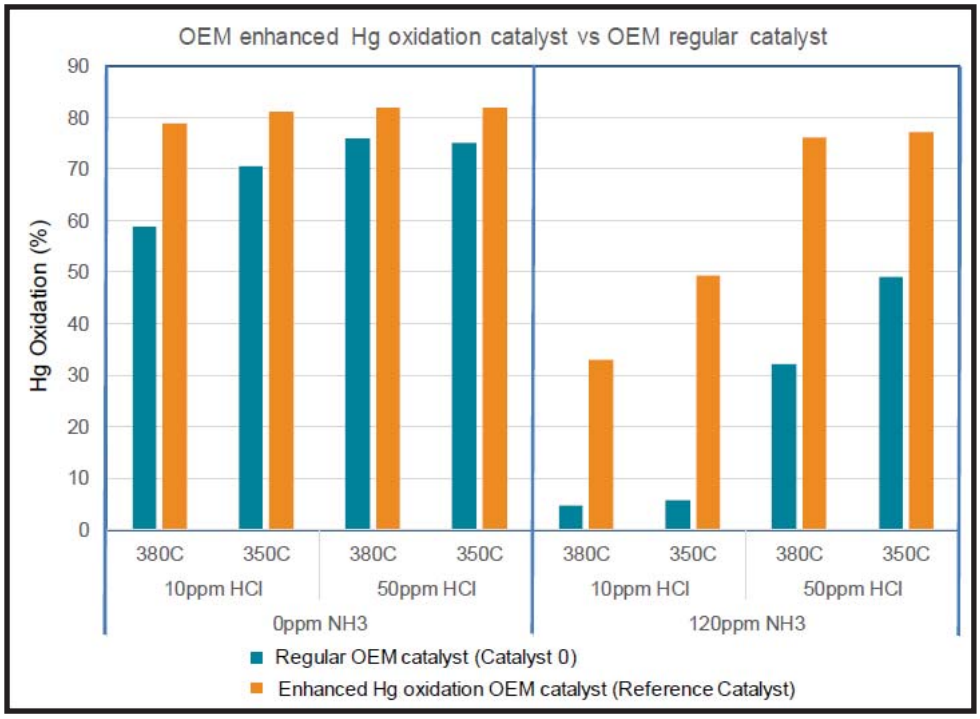

Figure 52: Hg oxidation study OEM enhanced Hg oxidation catalyst vs. regular catalyst.

- Can the Reference Catalyst be regenerated to achieve the same Hg oxidation performance?
- Can regular deactivated catalyst be regenerated to enhanced Hg oxidation (similar to reference catalyst)?

Aiming to answer the questions, the optimized regeneration method was used to regenerate and produce enhanced Hg oxidation catalyst. To reduce the cost of testing and save time, two of the test conditions were eliminated from the matrix (the low temperature high HCl tests). As can be seen in the data these test conditions didn't result in significantly different test results than the high temperature conditions. Preliminary test results demonstrated OEM enhanced Hg oxidation catalyst can be regenerated to achieve the same Hg oxidation level and a regular inventory deactivated catalyst can be regenerated to an enhanced Hg oxidation catalyst.

The test results shown in *Figure 53* on page 39.

Here, three treated catalysts were studied to compare to OEM Enhanced Hg oxidation catalyst (Reference Catalyst). They were:

- Catalyst 1 - An OEM enhanced Hg oxidation catalyst was cleaned and treated under the standard regeneration treatment process
- Catalyst 2 - An OEM enhance Hg oxidation catalyst was cleaned and treated under Cormetech proprietary optimized regeneration treatment process
- Catalyst 3 - A regular inventory deactivated catalyst was cleaned and treated under Cormetech proprietary optimized regeneration treatment process

The *Figure 53 on page 39* tells us:

- Under 0ppm NH_3 presenting condition, all Catalyst 1, 2, 3 show high Hg oxidation as similar as the reference catalyst
- Under 120ppm NH_3 concentration, Catalyst 1 resulted in a significantly lower Hg oxidation level than the reference catalyst. The Hg oxidation behaviors of Catalyst 1 is more like Catalyst 0
- And under 120ppm NH_3 concentration, Both Catalyst 2 and 3 resulted in an improved Hg oxidation level and as similar as or better than reference catalyst

CONCLUSION

OEM enhanced and regenerated catalyst samples were evaluated under a wide range of flue gas conditions the catalyst might be expected to perform under using a micro reactor and EPRI Hg Oxidation testing guidelines. The OEM en-

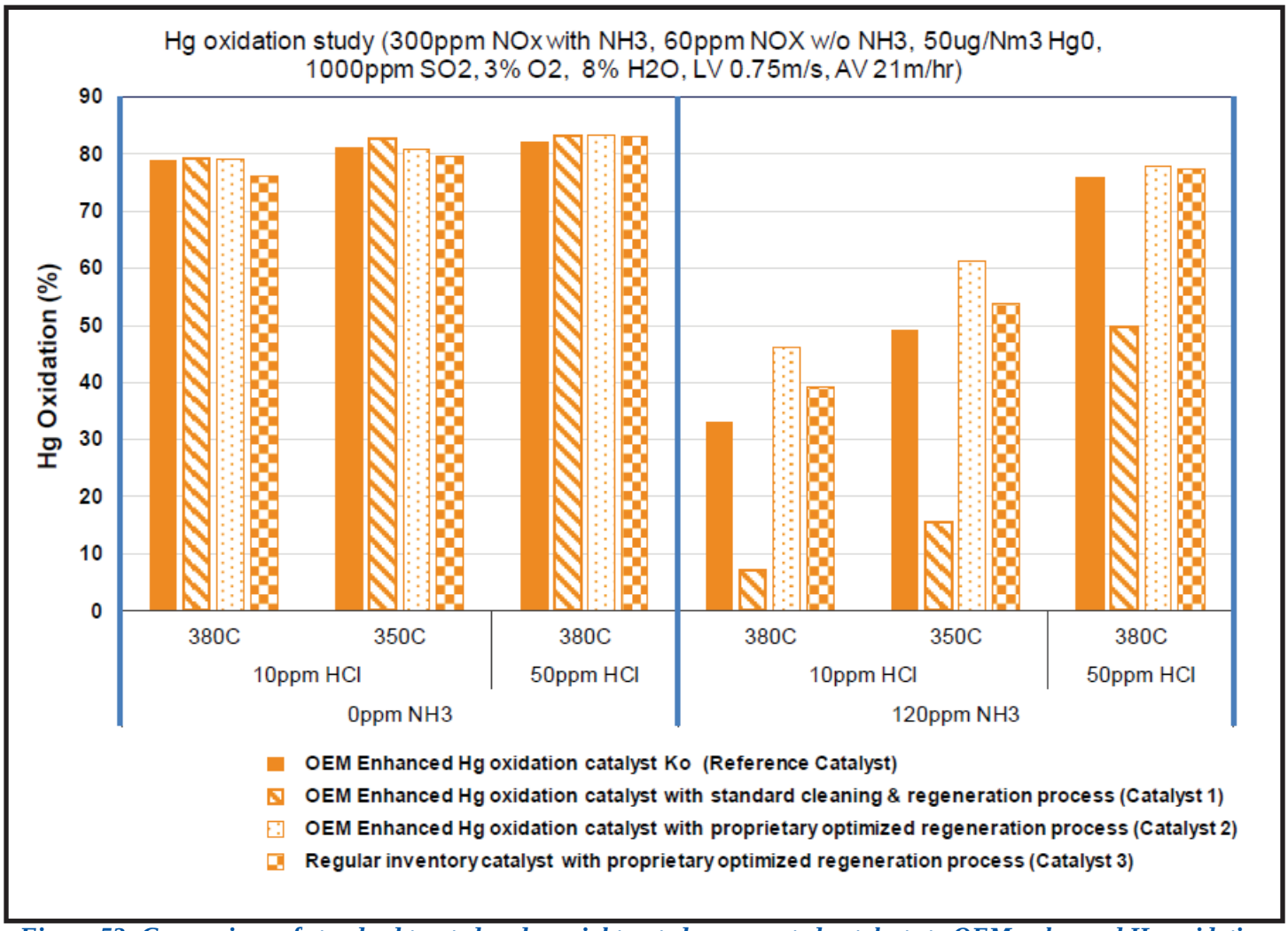

Figure 53: Comparison of standard treated and special treated regenerated catalysts to OEM enhanced Hg oxidation catalyst.

hanced Hg oxidation catalyst (reference catalyst) provided higher Hg oxidation levels than the standard OEM catalyst under conditions of high and low ammonia levels. The performance enhancement appears to be more significant at higher ammonia levels. To address utility concerns regarding the regenerability of these enhanced OEM Hg Oxidation catalysts, an optimized regeneration method was developed and demonstrated under lab conditions to meet OEM enhanced Hg Oxidation Catalyst performance levels.

References

1. Christopher Bertole, The SCR Toolbox for Mercury Emission Managemen, 2015 Reinhold NOx-Combustion Round Table Conference, The SCR Toolbox for Mercury Emission Managemen,
2. Division of Technology, Industry and Economics (DTIE) Chemicals Branch. Study on Mercury Sources and Emissions and Analysis of the Cost and Effectiveness of Control Measures; UNEP: Geneva, Switzerland, 2010.
3. Pirrone, N.; Cinnirella, S.; Feng, X.; Finkelman, B.R.; Friedli, R.H.; Leaner, J.; Mason, R.;
4. Mukherjee, B.A.; Stracher, G.; Streets, G.D.; Telmer, K. Mercury Fate and Transport in the
5. Global Atmosphere—Emissions, Measurements and Models; Springer: New York, NY, USA, 2009
6. Lee, B.J.; Lee, M.S.; Lee, Y.I. The characteristics of catalysts for mercury oxidation in thermal power plants. Proc. World Acad. Sci. Eng. Technol. 2008, 44, 256–257.
7. United Nations Environmental Programme: Minamata convention agreed by nations, Geneva/Nairobi, press release, 19.01.2013.
8. US EPA, Federal Register, 78 (2013) 24073–24094. <http://www.gpo.gov/fdsys/pkg/FR-2013-04-24/html/2013-07859.htm>.
9. K.C. Galbreath, C.J. Zygarlicke, Mercury speciation in coal combustion and gasification flue gases, Environ. Sci. Technol. 30 (1996) 2421–2426.
10. http://www.powermag.com/advanced-scr-catalysts-tune-oxidized-mercury-removal/
11. Hocquel, M. The Behaviour and Fate of Mercury in Coal-Fired Power Plants with Downstream Air Pollution Control Devices, VDI Fortschritt-Berichte, Vol. 251, VDI-Verlag, Düsseldorf, 2004.
12. A.A. Presto, E.J. Granite, Survey of catalysts for oxidation of mercury in flue gas, Environ. Sci. Technol. 40 (2006) 5601–5609.
13. H. Yang, Z. Xu, M. Fan, A.E. Bland, R.R. Judkins, Adsorbents for capturing mercury in coal-fired boiler flue gas, J. Hazard. Mater. 146 (2007) 1–11.
14. S. Chen, A.M. Rostam, R. Chang, Mercury removal from combustion flue gas by activated carbon injection: mass transfer effects, Prepr. Pap. Am. Chem. Soc., Div. Fuel Chem. 41 (1996) 442–446.
15. J. Wilcox, E. Rupp, S.C. Ying, D.H. Lim, A.S. Negreira, A. Kirchofer, F. Feng, K. Lee, Mercury adsorption and oxidation in coal combustion and gasification processes, Int. J. Coal Geol. 90 (2012) 4–20.
16. N. Omine, C. E. Romero, H. Kikkawa, S. Wu, and S. Eswaran, "Study of

elemental mercury re-emission in a simulated wet scrubber," Fuel, vol. 91, no. 1, pp. 93–101, 2012.
17. J. Wo, M. Zhang, X. Cheng, X. Zhong, J. Xu, and X. Xu, "Hg2+ reduction and re-emission from simulated wet flue gas desulfurization liquors," Journal of Hazardous Materials, vol. 172, no. 2-3, pp. 1106–1110, 2009.
18. J. C. Chang and S. B. Ghorishi, "Simulation and evaluation of elemental mercury concentration increase in flue gas across a wet scrubber," Environmental Science & Technology, vol. 37, no. 24, pp. 5763–5766, 2003.
19. D. Pudasainee, S.J. Lee, S.H. Lee, J.H. Kim, H.N. Jang, S.J. Cho, Y.C. Seo, Effect of selective catalytic reactor on oxidation and enhanced removal of mercury in coal-fired power plants, Fuel 89 (2010) 804–809.
20. V.I. Marshneva, E.M. Slavinskaya, O.V. Kalinkina, G.V. Odegova, E.M. Moroz, G.V. Lavrova, A.N. Salanov, The influence of support on the activity of monolayer vanadia–titania catalysts for selective catalytic reduction of NO with ammonia, J. Catal. 155 (1995) 171–183.
21. Karin Madsen, Joakim Reimer Thøgersen, Flemming Frandsen and Anker Degn Jensen. Mercury oxidation over selective catalytic reduction (SCR) catalysts. Presented at Power-Gen Europe 2012, 12-14 June, Cologne, Germany
22. T. Schwämmle, A. Hartung, B. Heidel, G. Scheffknecht: A study on the interaction of mercury oxidation and NOx-reduction by newly developed high-performance SCR-DeNOx-Catalysts, Air Quality IX, Arlington, VA, October 21-23, 2013

STEAG SCR-Tech acquires Cormetech

On November 1, 2017, STEAG SCR-Tech, Inc., an SCR catalyst regeneration service, acquired CORMETECH, Inc., a manufacturer of high-quality environmental catalysts and services for the power, marine, industrial-process, refinery, and petrochemical markets. The two companies merged their businesses, adopting the 28 year old CORMETECH name.

Mike Mattes will be the President and CEO of the newly formed company with Dave Morris as the CFO. Senior Vice Presidents will be Chris DiFrancesco (& CTO), Scot Pritchard (Sales Engineering) and Scott Daughtery (Business Development & Manufacturing).

The former CORMETECH Company was formed in 1989 from the equity ownership of MHI and Corning. It's catalyst technologies uniquely benefit from the ceramic extrusion technology of Corning Incorporated and SCR system design, engineering, and experience of MHI. The new Cormetech will now be a joint equity venture of STEAG GmbH and Energy Capital Partners. STEAG brings to the table years of German experience regenerating catalyst. Energy Capital Partners is a private equity firm focused on investing in energy infrastructure.

Operating Challenges of Existing SCR and DSI Systems

Written by Suzette Puski, Babcock Power Inc.

INTRODUCTION

With dispatch requirements resulting from changing generation portfolios, coal fired generating units are facing challenges running Selective Catalytic Reduction (SCR) and Dry Sorbent Injection (DSI) systems to meet emissions requirements. Maintaining flue gas and temperature distribution is important to maintain permitted emissions. Equally important is maintaining the marketability of fly ash, minimizing ammonia and sorbent feed, and reducing operating and maintenance (O&M). The keys to addressing these challenges are a comprehensive understanding of the design and operation of the equipment and technology and expertise to apply solutions to resolve these issues. Original Equipment Manufacturers (OEMs) that supply boiler and Air Quality Control Systems (AQCS) systems understand the entire process and process impacts across the system and can partner with owners to find solutions to these challenges.

OPERATING CHALLENGES

Renewable energy systems are increasingly being used for electricity generation. These technologies often have fluctuation in power output over short periods of time. Conventional utilities are often used to make up the power difference. This creates a challenge for utilities as systems are required to operate with more frequent and larger load swings compared to historic operation. Systems are also required to further reduce minimum load conditions from 50% to as low as 30% MCR. Variability in operation can lead to an increase in some flue gas emissions such as NOx. Low flue gas temperatures at reduced loads make it difficult to maintain AQCS systems in service.

Adding to the challenge of maintaining emissions at variable load conditions is variability in fuel sourcing and fuel blends. Higher sulfur fuels result in higher SO_3 formation. Controlling ammonia slip with transitional NOx emissions and higher SO_3 formation is important to maintain NOx emissions, minimize ammonium bisulfate formation and scaling, and optimize air heater operation (efficiency and pressure drop).

Tighter budgets for staff and O&M and less frequent/shorter outages add to the challenge to minimize reagent feeds under all operating and fuel conditions and maintain equipment in service that is aging and often wears faster with cyclic operation.

Addressing these challenges require:

- Maintaining emissions at lower loads and through constant load swings
- Optimizing operation with variable fuels including gas and coal/gas blends
- Maintaining/increasing reliability with fewer outages
- Understanding and evaluating entire process and impacts of changes across entire process systems

MIXING TECHNOLOGY

The first step to address challenges facing utilities is to improve distribution of flue gas, ammonia and sorbents. For SCR, mixing is completed upstream of the catalyst reaction zone. There is no mixing in the catalyst zone. Poor mixing results in high NOx emissions, high ammonia slip, ammonium bisulfate formation, particulate accumulation, higher pressure drop if additional catalyst is required and low load restrictions due to poor temperature distribution. Figure 54

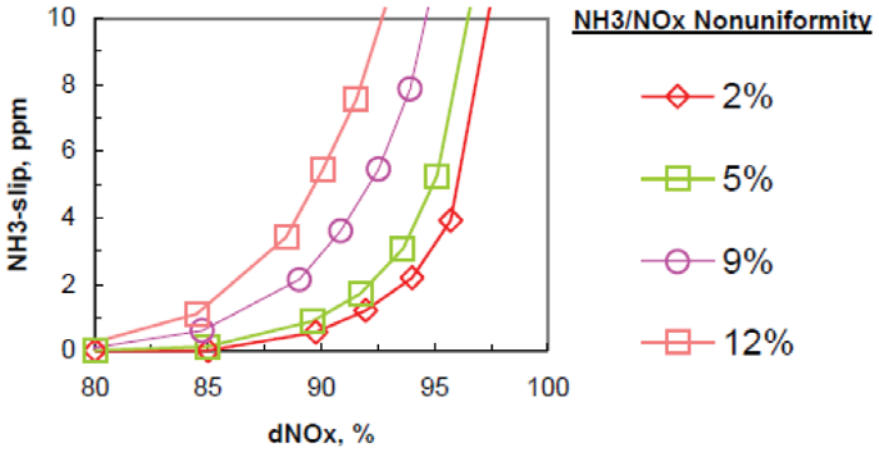

Figure 54: NOx removal versus Ammonia slip (from Muzio, Smith, and Martinez, "New Tools for Diagnosing SCR Performance Issues")

shows effect of mal-distribution on catalyst performance on a coal-fired unit. As NOx removal efficiency requirements increase, maintaining mixing is important to minimize ammonia slip.

Replacing traditional ammonia injection systems with static mixers reduces the number of lances and injection nozzles required. Reducing the number of lances reduces the frequency of tuning required and maintenance related to plugged nozzles.

However, maintaining distribution of ammonia is not always enough to optimize SCR operation. Tuning the ammonia injection system at full load and one fuel condition is not always adequate at reduced loads or other fuel conditions. Removing mal-distribution upstream of ammonia injection has been demonstrated to be just as important to account for firing and draft system variations.

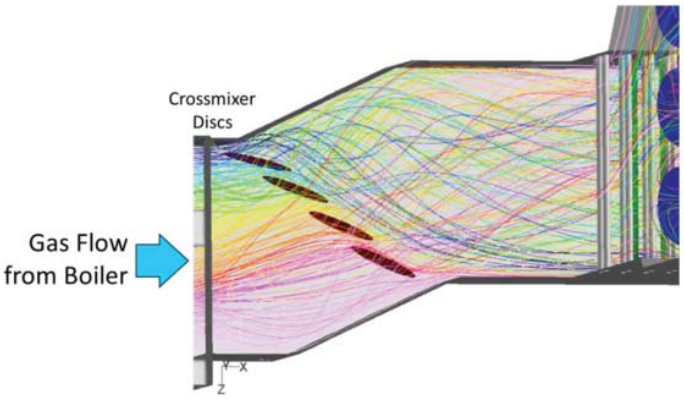

Figure 55: CFD Model Demonstrating Achieving Homogeneous Distribution Upstream of Injection

Figure 55 is a CFD model to visually demonstrate how static mixers can be used to maintain distribution of NOx, flue gas temperature, and particulate upstream of ammonia injection under variable fuel and flue gas flows.

Figure 56 is an example of utilizing static mixers to maintain temperature distribution on a large 650 MW coal-fired unit in North Carolina. Temperature measurements across a 49-point grid provided data demonstrates temperature distribution is maintained repeatedly across the operating load range. Minimizing the temperature deviation is important for reduced load operation. If the catalyst minimum temperature can be reduced due to effective mixing, the SCR can remain in service at lower loads prior to requiring a means to increase the flue gas temperature with an economizer bypass or an induct burner.

Static mixers can reduce the effect of maldistribution at the interface point to the SCR. Figure 57 on page 43 is an example of ammonia-to-NOx mixing being maintained across the load range with different fuel types utilizing static mixers on a 550 MW unit in Kentucky.

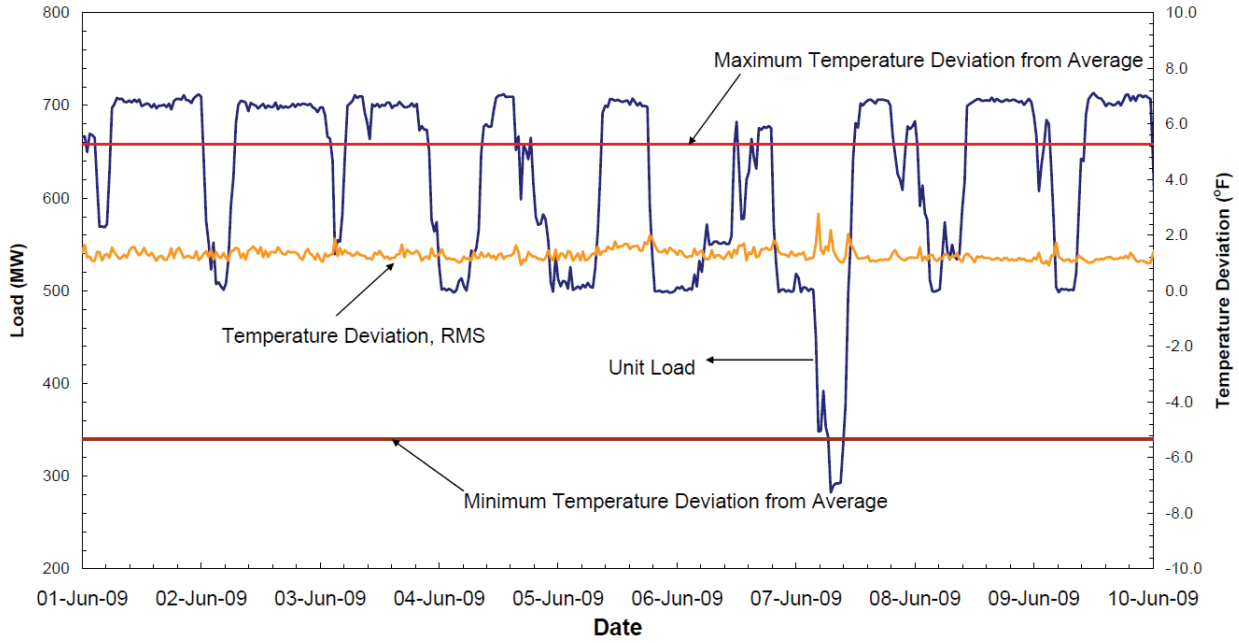

Figure 56. Temperature Distribution at Catalyst Face 48'-2" x 41'-7" during Load Swings on a Coal-Fired Unit in North Carolina

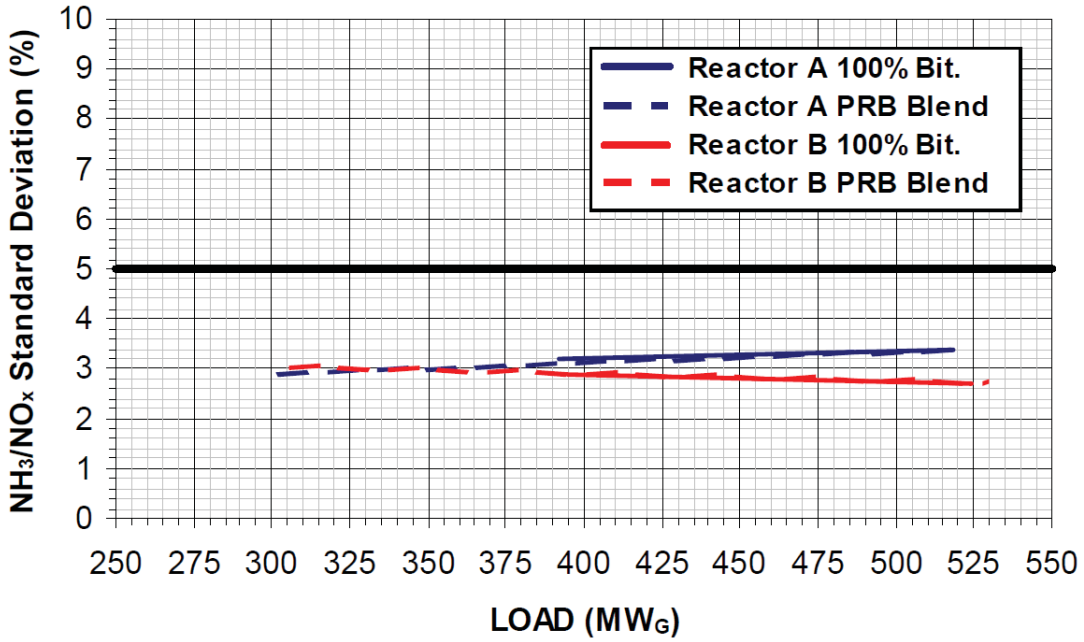

Figure 57. Homogenous Mixing with Bituminous Coal and Powder River Basin Coal Blends Across the Operating Load Range on a 550 MW Unit in Kentucky

DSI systems are utilized to remove pollutants including SO_2, SO_3, Hg, and HCl dependent on flue gas conditions, the type of sorbent, and location of the injection system. DSI mixing is completed at the injection point. Poor mixing results in longer residence time requirements (longer lengths of duct), high emissions, and high reagent consumption.

At several plants the DSI system is installed between the SCR and the airheater to remove SO_3 to reduce potential for ammonium bisulfate scaling. The residence time is often short in this area of ductwork and distribution with a traditional injection grid does not provide adequate residence time to remove SO_3. Distribution with a traditional injection grid system is also flue gas flow dependent. For example, at reduced flue gas flows sorbent may drop out of the flue gas stream.

Static mixers can be utilized to disperse sorbent without the requirement of an injection grid and a multitude of small nozzles. The mixers create vortexes to fully disperse sorbent across a short section of duct. The dispersion is independent of flue gas flow.

With static mixing full coverage is achieved in a relatively short section of ductwork and is independent of flue gas flow. Figure 58 on page 44 shows sorbent distribution and residence time from model results for a DSI upgrade project at 25, 50 and 75% load respectively from left-to-right for a utility in Tennessee. Full mixing is achieved upstream of the duct split. Maintaining distribution across a short section of duct throughout the load range is beneficial for SCR systems to achieve mixing upstream of the catalyst face and DSI systems which are often located in the short section of ductwork between the SCR and air heater.

A poor performing DSI system for SO_3 removal can also impact the performance of a downstream injection system utilizing activated carbon for mercury removal. Activated carbon reacts with SO_3 in the flue gas increasing reagent consumption. Hydrated lime is a 5 to 10 times more economical reagent for SO_3 removal. If an activated carbon system for mercury removal is installed downstream of a DSI system for SO_3 removal, utilizing static mixers to maximize SO_3 removal upstream of activated carbon injection reduces activated carbon consumption.

Relocating the DSI system upstream of the SCR has several benefits including:

- Utilizing the same set of static mixers for ammonia and lime injection
- Reducing SO_3 to the SCR which reduces the minimum operating temperature of the catalyst for reduced load operation
- Reducing the formation of ammonium bisulfate scaling and improving air heater efficiency

Scaled physical flow modeling is often used to model turbu-

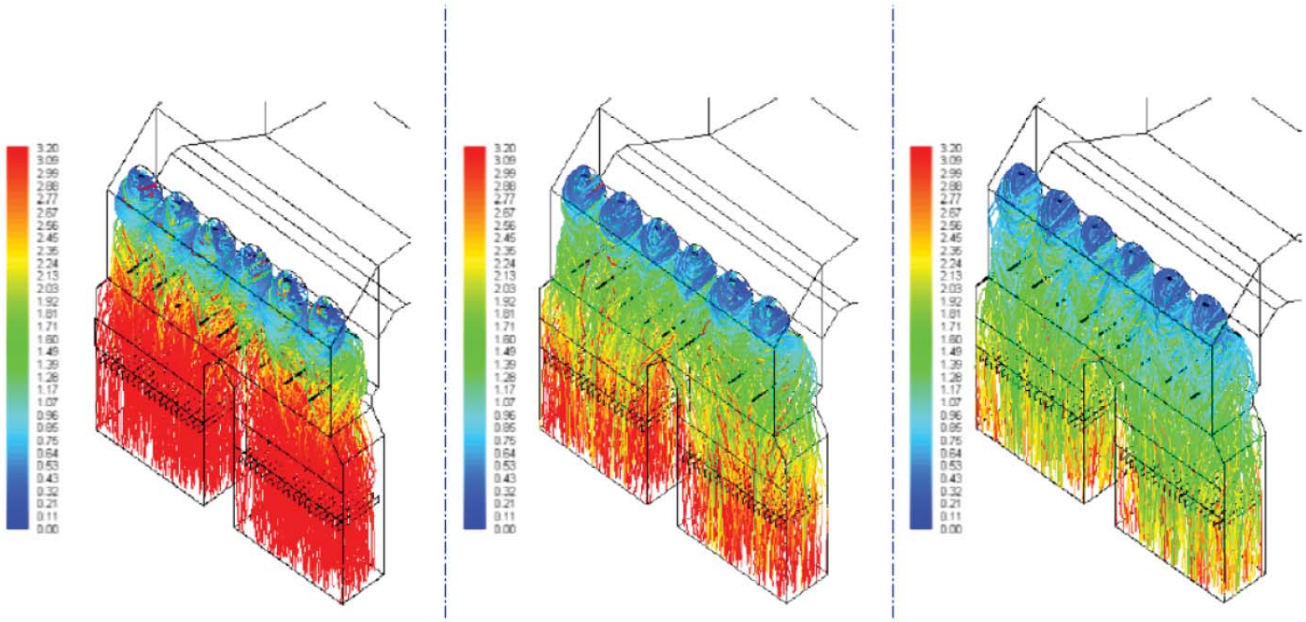

Figure 58: Full Mixing Achieved at 25%, 50%, and 75% Load from Left to Right for DSI upgrades at a Utility in Tennessee

lent flows and to understand particulate distribution under variable flue gas flow conditions to prevent buildup in sections of ductwork or across the catalyst face. If particulate or sorbent suspension cannot be maintained at low loads, it is important to understand at what flue gas flows and where particulate or sorbent will drop out and design the system to re-entrain the particulate and sorbent at higher flue gas flows to prevent accumulation. CFD modeling can be used to model fallout but not re-entrainment.

Load swings and higher NOx removal require NOx monitoring upstream and downstream of the SCR to be able to maintain emissions during transitional periods. Feed forward logic is used to determine ammonia feed based on flue gas flow, measured inlet NOx and the NOx emissions set point. Feedback logic adjusts feed based on measured outlet NOx emissions. The time lag of using the stack NOx analyzer can be long and would require maintaining a higher removal set point to account for dips during transition periods. Uniform mixing has the benefit of minimizing the number of NOx analyzers required to monitor inlet and outlet NOx compared to traditional ammonia grid systems where multiple inlet and outlet NOx analyzers are required across the ductwork.

Improving mixing with static mixers for SCR and DSI systems provides the following benefits:

- Reduce effects of unit firing & flow configurations
- Produce homogenous flue gas at the catalyst face
- Reduce residence time requirements
- Reduce variability upstream of ammonia or sorbent injection
- Maintain ash entrainment and distribution
- Improve flue gas temperature distribution
- Maintain mixing at low load operation
- Reduce ammonium bisulfate scaling/optimize air heater efficiency

EXAMPLES of SYSTEM UPGRADES

Increasing Reliability and Reducing O&M

SCR systems on two 500 MW boilers firing high sulfur bituminous coal at a utility in Indiana had several operating issues including:

- Leaks from the ammonia vaporization system
- Pluggage of the ammonia injection nozzles with ash
- Fouling of tuning valves and piping with ammonia compounds
- High ammonia slip

The ammonia injection grid required frequent tuning and cleaning. When the tuning was completed to match ammonia to incoming NOx profile, the profiles changed with load and boiler operation. Tuning the reactor was also made complicated with 40 manual tuning valves and 780 nozzles per reactor.

Physical modeling was completed to add static mixers to improve mixing of the flue gas prior to ammonia injection. Additional mixers coupled with larger open lances replaced

	Unit 1	Unit 2
Inlet NOx, St Dev		
Baseline Test	9.7%	7.5%
After Upgrade	3.8%	3.2%
NH_3/NOx, min/max		
Baseline Test	-28/+21%	-29/+21%
After Upgrade	-10.5/+8.4%	-8.5%/+7.9%
NH_3 Slip		
Baseline Test	>10 ppmv	>10 ppmv
After Upgrade	0.13 ppmv	0.22 ppmv

Figure 59: SCR NOx and NH3/NOx Mixing Profile

the unreliable ammonia injection grid. Tuning requirements were reduced to every other year and the duration for tuning also shortened significantly. Pluggage of the ammonia injection system was eliminated and ammonia slip reduced along with ammonium bisulfate scaling. The ammonia vaporization system was replaced with direct ammonia injection to eliminate O&M with the vaporization system. The improvements in NOx distribution and ammonia to NOx mixing are summarized in Figure 59. Inlet NOx distribution was improved to the ammonia injection system. Ammonia/NOx mixing was significantly improved and ammonia slip significantly reduced. The catalyst was not replaced when these improvements were completed and did not influence results.

Overall the upgrade of the SCR accomplished:

- Minimizing ammonia slip while maintaining NOx emissions
- Reducing/eliminating scaling in nozzles and downstream in the air heater

Figures 60 and 61 show before and after photos of the ammonia injection system.

Figure 60. Ammonia Injection Grid (AIG) with 40 Valves (Left) Reduced to 8 Valves (Right)

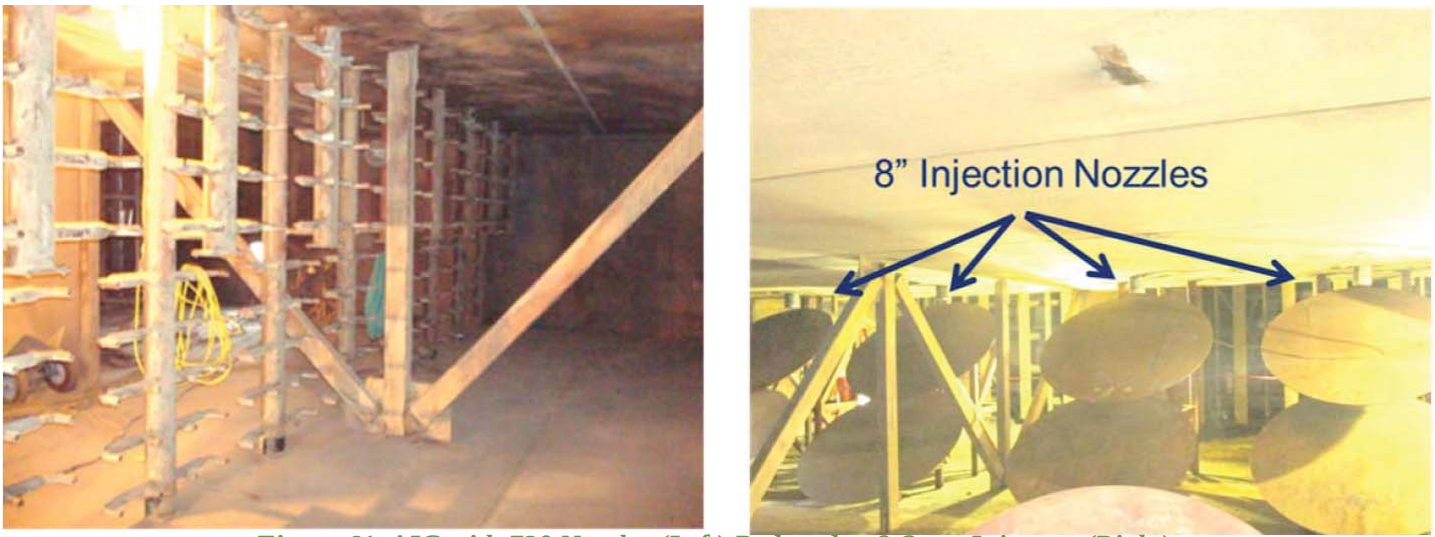

Figure 61. AIG with 720 Nozzles (Left) Reduced to 8 Open Injectors (Right)

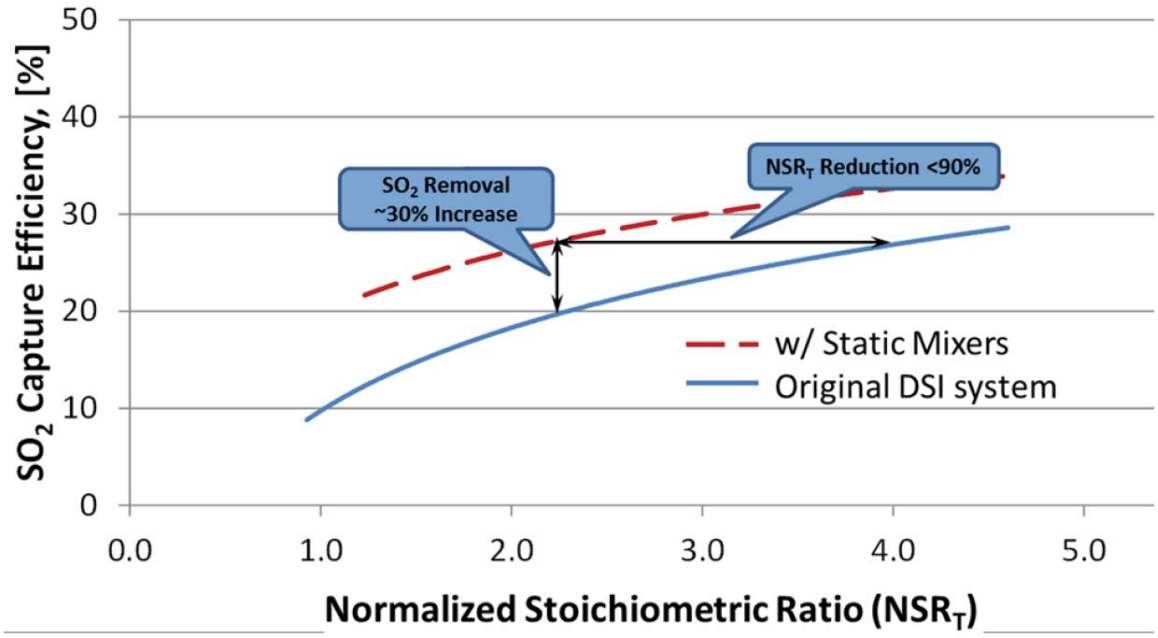

Figure 62. DSI Upgrade Results for a 125 MW Unit in Tennessee

- Reducing O&M associated with cleaning and tuning the SCR and cleaning the air heater
- Eliminating O&M associated with the vaporization system
- Optimizing pressure drop and performance across the air heater
- Optimizing ash distribution
- Additionally, the system improved the mixing and distribution of the sodium-based solution injection system upstream of the SCR for SO_3 removal

Upgrade DSI system

Coupling static mixers with sorbent injection allowed for fewer, larger lances to distribute sorbent in shorter sections of duct. Removal efficiencies are increased coupled with a decrease in sorbent usage. Figure 62 shows the improvement in SO_2 capture utilizing static mixers at a plant in the Southeast. To achieve the same removal without mixers would require almost double the hydrated lime feed

The cost savings achieved for the DSI upgrade is summarized in Figure 63 below. A secondary benefit was increasing HCl removal 15% at the same lime feed rate.

Capacity	175 MW
Add Static Mixers	$400,000
Hydrated Lime Savings	$325,000/year at 70% capacity

Figure 63:. Savings Achieved on DSI Upgrade Utilizing Static Mixers

EVALUATE ENTIRE PROCESS and IMPACTS of CHANGES

Sometimes a lot of focus is maintained on keeping equipment in service without an understanding of upstream and downstream operations. An example was mentioned earlier when an activated carbon system is installed downstream of a hydrated lime sorbent system. Improving the hydrated lime system also benefits the activated carbon system by reducing activated carbon consumption used to remove SO3.

Adding a Large Particle Ash (LPA) screen at the economizer hopper can reduce ash accumulation on the catalyst face while utilizing the existing ash removal system.

SUMMARY

It is important to understand process and process impacts across the system to properly address the challenges facing utilities and meet future regulations. Original Equipment Manufacturers (OEMs) supplied the original technology and equipment based on the conditions at the time of installation. With changing conditions and a better understanding of operation, OEMs are best qualified to optimally evaluate the process and process impacts to provide the most cost effective, environmentally responsible generation solutions available today. Detailed specifications are not required for this type of work and tend to be difficult and expensive to develop. An OEM, that understands the entire process and will partner in a collaboratively fashion with the owner, will develop the solution from identification to installation that provides an overall approach.

For further information, contact

For further information contact
Suzette Puski at mailto:SPuski@babcockpower.com

BIOGRAPHY

Suzette Puski started working in the power industry in 1991 after graduating in chemical engineering from Purdue University. She evaluated AQCS proposals, attended plant start-ups and completed optimization testing. She then transferred to R&D in manufacturing where she worked as a process engineer scaling up product from R&D to pilot-scale to the manufacturing plant. Over the last 12 years Suzette has worked for Babcock Power starting as a process engineer completing engineering, commissioning and startups, and optimization of AQCS systems. She now works in proposals where she uses her plant experience to provide practical solutions to the power industry.

Babcock Power
ENVIRONMENTAL
a Babcock Power Inc. company

Who We Are

The Worldwide Pollution Control Association (WPCA) has assembled a group of people and companies who are experts at some aspect of pollution control. In addition, the WPCA has organized a user advisory board who can give this group direction and assistance in performing service to pollution control business throughout the world.

Our Mission

The mission of the WPCA is to enhance technical communication through seminars, technical journals and a website. The WPCA is a non-profit organization and our members and advisors need to be motivated by a desire to see the pollution control community make world wide technical progress through improved technical communication.

Who Directs the WPCA?

The WPCA is a partnership which includes system/equipment/services suppliers, consultants and users. The WPCA President, Vice President and Advisory Committee are equipment users. The Corporate Sponsors and Board of Directors are suppliers. Together they develop annual seminars and events to achieve their goal of better technical communication for users of air pollution control systems.

How do I become a Member of the WPCA?

In order to be a WPCA member, you must be an end user of pollution control equipment. When you register on-line for any WPCA sponsored seminar, you automatically become a member. If you would like to join, but cannot attend a seminar at this time, please download and send in the Registration Form at the top of the members list at www.wpca.info. You will then be emailed regarding upcoming events and sent future copies of the WPCA News.

WPCA Corporate Sponsors

WPCA Chairman
Susan Reinhold,
CEO
Reinhold Environmental Ltd.
3850 Bordeaux Drive, Northbrook, IL 60062 USA
Email: sreinhold@reinholdenvironmental.com

WPCA Secretary
Sharon Sjostrom,
Chief Product Officer, Market Strategy
ADA-ES, Inc.
9135 S. Ridgeline Blvd., Ste 200,
Highlands Ranch, CO 80129 USA
Email: sharons@adaes.com

WPCA Treasurer
Robert Mudry,
President
Airflow Sciences Corporation
12190 Hubbard Street, Livonia, MI 48150 USA
Email: rmudry@airflowsciences.com

WPCA Vice President
Blake Stapper,
Business Manager
AECOM
9400 Amberglen Blvd., Austin, TX 78729 USA
Email: blake.stapper@aecom.com

Clayton Erickson,
Manager, Process Engineering
Babcock Power Inc.
5 Neponset Street, Worcester, MA 01606 USA
Email: cerickson@babcockpower.com

Allen Kephart,
President
CleanAir Engineering
110 Technology Dr., Pittsburgh, PA 15275
Email: akephart@cleanair.com

Mike Mattes
CEO
Cormetech
304 Linwood Rd, Ste.102, Kings Mountain, NC 28086 USA
Email: m.mattes@steagscrtech.com

Mike Allen,
Senior Sales Manager
CLARCOR Industril Air
11501 Outlook St., Ste. 100,
Overland Park, KS 66211 USA
Email: mike.allen@clarcor.com

Wesley McKenzie,
VP Technology
Southern Environmental, Inc.
6690 West Nine Mile Rd., Pensacola, FL 32526
Email: wmckenzie@sei-group.com

Curt Biehn,
Director of Marketing
Mississippi Lime
3870 S. Lindbergh Blvd., St. Louis, MO 63127
Email: crbiehn@mississippilime.com

Paul Ford,
President
Redkoh Industries
300 Valley Road, Hillsborough, NJ 08844 USA
Email: paul.ford@redkoh.com

Mitch Lund,
Product Manager
Nol-Tec Systems, Inc.
425 Apollo Drive
Lino Lakes, MN 55014 USA
Email: mitchlund@nol-tec.com

Mike Volker
Business Development
Stock Equipment Company
16490 Chillicothe Road,
Chagrin Falls, OH 44023 USA
Email: m.volker@schenckprocess.com

Nate White,
Director, Air Emission Control
Umicore Catalyst USA
5510 Morris Hunt Dr.,
Fort Mill, SC 29708 USA
Email: Nathan.White@am.umicore.com

Kevin McDonough,
VP Sales & Marketing
United Conveyor Corporation
2100 Norman Drive West
Waukegan, IL 60085 USA
Email: kevinmcdonough@unitedconveyor.com

Jake Blattman,
Industrial Sales Manager
WesTech
3665 S. West Temple
Salt Lake City, UT 84115 USA
Email: jblattman@westech-inc.com

Paul Leanza,
Business Development Manager
KraftPowercon
112 West Gregory Street
Pensacola, FL 32502 USA
Email: Paul.Leanza@kraftpowercon.com

Max Swoboda,
Business Development Manager
Evoqua
1500 Toney Drive
Huntsville, AL 35802 USA
Email: max.swoboda@evoqua.com

WPCA Officers

WPCA President
Melissa Allen, Environmental Systems Manager,
TVA

WPCA Vice President
Michael O'Connor, Program Manager
Dynegy

WPCA Advisors

Greg Betenson,
Principal Engineer,
PacifiCorp

Melanie McCoy,
Superintendent
Sebewaing Light & Power

Ebrahim Patel,
Senior Consultant - APC,
ESKOM-GTD

Bruce Salisbury,
Engineering Supervisor,
Arizona Public Service

Scott Williams,
Principal Engineer,
Duke Energy

Darren Hanby,
Principal Engineer,
AEP

Brandon Bettinger
Chemical Engineer
East Kentucky Power Cooperative

Kayla Pauvlinch
Engineer IV
FirstEnergy

Logan Waller
Chemical Engineer
Louisville Gas & Electric